

AMERICAN UNIVERSITY OF BEIRUT

MODEL-BASED DYNAMIC CONTROLLER OF
PERSONALIZED VENTILATION FOR THERMAL
COMFORT IN NATURALLY VENTILATED SPACES.

by

DALIA ALI GHADDAR

A thesis
submitted in partial fulfillment of the requirements
for the degree of Master of Engineering
to the Department of Mechanical Engineering
of the Maroun Semaan Faculty of Engineering and Architecture
at the American University of Beirut

Beirut, Lebanon
September 2020

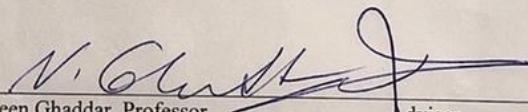
AMERICAN UNIVERSITY OF BEIRUT

MODEL-BASED DYNAMIC CONTROLLER OF PERSONALIZED
VENTILATION FOR THERMAL COMFORT IN NATURALLY
VENTILATED SPACES.

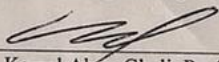
by

DALIA ALI GHADDAR


Approved by:



Dr. Nesreen Ghaddar, Professor
Mechanical Engineering
Advisor



Dr. Kamel Abou Ghali, Professor
Mechanical Engineering
Co-Advisor



Dr. Joseph Zeaiter, Professor
Chemical Engineering
Member of Committee

Date of thesis defense: September 7, 2020

THESIS, DISSERTATION, PROJECT RELEASE FORM

Student Name: Ghaddar Dalia Ali
Last First Middle

Master's Thesis Master's Project Doctoral Dissertation

I authorize the American University of Beirut to: (a) reproduce hard or electronic copies of my thesis, dissertation, or project; (b) include such copies in the archives and digital repositories of the University; and (c) make freely available such copies to third parties for research or educational purposes.

I authorize the American University of Beirut, to: (a) reproduce hard or electronic copies of it; (b) include such copies in the archives and digital repositories of the University; and (c) make freely available such copies to third parties for research or educational purposes after:

- One ---- year from the date of submission of my thesis, dissertation, or project.
- Two ---- years from the date of submission of my thesis, dissertation, or project.
- Three ---- years from the date of submission of my thesis, dissertation, or project.

Dalia

10-9-2020

Signature:

Date:

ACKNOWLEDGMENTS

The authors would like to acknowledge the financial support of the American University of Beirut – University Research Board – Grant award no. 103780.

AN ABSTRACT OF THE THESIS OF

Dalia Ali Ghaddar for

Master of Engineering
Major: Mechanical Engineering

Title: Model-based dynamic controller of personalized ventilation for thermal comfort in naturally ventilated spaces

This work aims to develop an accurate correlation using a modeling methodology to predict thermal comfort (TC) as function of occupant physiological and environmental parameters for a space that relies on the hybrid natural ventilation (NV) and personalized ventilation (PV) cooling system. Multivariable linear regression was adopted to develop the TC correlation while retaining variables based on the significance and interdependency. The correlation was found to be dependent on indoor temperature (T_{indoor}), relative humidity (RH), facial temperature (T_{facial}) and its rate of change (dT_{facial}/dt). Sample data from the observations used in developing the correlation and outside-data were utilized to compare actual and predicted TC results over a scale from -4 (very uncomfortable) to +4 (very comfortable). The reported standard error in estimating TC was 0.4 with a maximum deviation of about 0.8.

The TC correlation is then utilized in developing dynamic controllers for NV-PV systems. A PV unit, autonomously controlled, in a NV office space was developed to maintain acceptable TC at all times of operation. The NV-PV controller robustly adjusts the PV supply temperature (T_{SPV}) at the occupant set flow rate based on the developed TC correlation. The target TC level that the controller should attain at all times is between 0.5 and 1 based on Zhang's TC scale (just comfortable to slightly comfortable). The developed controller was tested in a case study of an office space in Beirut's climate (with indoor temperature ranging between 25 and 33 °C, and RH between 60 and 80 %). It was shown that the NV-PV controller can dynamically adjust T_{SPV} to maintain acceptable TC between 0.5 and 1 at all times.

CONTENTS

ACKNOWLEDGMENTS.....	v
ABSTRACT.....	vi
LIST OF ILLUSTRATIONS.....	xi
LIST OF TABLES.....	xii
NOMENCLATURE.....	ix
Chapter	
I. INTRODUCTION.....	1
II. TC CORRELATION METHODOLOGY.....	6
A. Methodology for developing the <i>TC</i> correlation and its influential variables	6
B. The bioheat model.....	10
C. Zhang (2003) <i>TC</i> model.....	11
D. The IES-VE NV office space model.....	12
E. Simulated cases for development of <i>TC</i> correlation.....	13
F. Development and assessment of <i>TC</i> correlation.....	17
III. NV-PV CONTROLLER METHODOLOGY.....	18
A. Applicability of the developed <i>TC</i> correlation.....	29
B. NV-PV dynamic controller	20

IV. TC CORRELATION RESULTS.....	24
A. Sample of actual data collected for <i>TC</i> correlation development.....	24
B. Multivariable linear regression analysis.....	28
C. <i>TC</i> correlation evaluation results	31
V. NV-PV CONTROLLER RESULTS.....	39
A. Effect of transient changes in T_{SPV} on <i>TC</i> results	39
B. PID control parameters using trial and error.....	40
VI. CASE STUDY.....	42
A. Case study for real-time implementation and testing of NV-PV dynamic controller	42
B. Case study evaluation results	44
VII. CONCLUSION.....	48
BIBLIOGRAPHY.....	45

NOMENCLATURE

dT_{facial}/dt	: rate of change of facial temperature, °C/min
dT_{indoor}/dt	: rate of change of indoor temperature, °C/min
dT_{wrist}/dt	: rate of change of wrist temperature, °C/min
<i>HVAC</i>	: Heating, Ventilation and Air Conditioning area
<i>IES-VE</i>	: Integrated Environmental Solutions-Virtual Environment
<i>NV</i>	: Natural ventilation
<i>PID</i>	: Proportional Integral Derivative
<i>PV</i>	: personalized ventilation
Q_{SPV}	: personalized ventilator supply flow rate, L/s
<i>RH</i>	: relative humidity, %
<i>TC</i>	: thermal comfort
T_{facial}	: facial temperature, °C
T_{indoor}	: indoor temperature, °C
<i>TMY</i>	: Typical Meteorological Year
T_{SPV}	: personalized ventilator supply temperature, °C
$T_{SPV-set}$: personalized ventilator set supply temperature, °C
$(T_{SPV})_k$: feedback value of present T_{SPV} , °C
T_{wrist}	: wrist temperature, °C
K_p	: proportional gain
K_i	: integral gain
K_d	: derivative gain

- N : total number of iterations
- E_k : temperature difference between $(T_{SPV})_k$ and $T_{SPV-set}$ of this iteration
- E_{k-1} : temperature difference between $(T_{SPV})_k$ and $T_{SPV-set}$ of previous iteration
- $\sum_{t=0}^k E_t$: integral error

Greek symbols

- α : intercept of the line
- β : linear slope coefficient

ILLUSTRATIONS

Figure	Page
1. Schematic of the NV-PV system in an office space.....	7
2. Proposed methodology for developing a TC correlation under NV-PV system.....	9
3. Schematic of the multi-segmented human body as adopted in the bioheat model.....	11
4. Flow chart of the developed methodology.....	19
5. Transient T_{SPV} profile under uniform indoor conditions.....	20
6. NV-PV dynamic PID controller	22
7. NV-PV dynamic controller flowchart	24
8. Sample of collected data of skin temperatures, indoor conditions and their rate of change under August indoor condition transients	27
9. Sample of collected data of skin temperatures, indoor conditions and their rate of change under metabolic rate transients	28
10. Scatter plot for predicted versus actual TC corresponding to all the observations under steady and transient conditions.....	31
11. Comparison between the predicted and actual TC values under transient conditions of metabolic rate for 3 observations.....	35
12. Comparison between the predicted and actual TC values under transient conditions of metabolic rate for 3 outside-data sets.....	36
13. Effects of transient changes in T_{SPV} on T_{facial} and TC	40
14. Tuning PID controller for a specific case.....	41
15. Schematic showing the plan view of the simulated office space.....	43
16. Indoor conditions (T_{indoor} and RH) over the working hours for the month of August.....	45
17. The variation in T_{SPV} as well as T_{facial} and (b) the comparison between the predicted and the actual TC for a typical working day of August.....	47

TABLES

Table		Page
1.	Typical T_{indoor} and RH during the four summer months.....	13
2.	Typical average T_{indoor} and RH during the morning, mid-day and afternoon of the four summer months (Doctor-Pingel et al. 2019; Khalil et al. 2020).....	15
3.	Regression Statistics and ANOVA.....	30
4.	Evaluation of the TC correlation using 6 outside-data points representing steady state situations.....	32
5.	Benchmark of results for the TC correlation.....	38
6.	Indoor space and PV conditions to tune the PID controller.....	41
7.	Metabolic rate profile over the working hours adopted in each of the case studies.....	44

CHAPTER I

INTRODUCTION

HVAC systems account for more than 40% of energy consumption in buildings to maintain acceptable indoor environments that provide thermal comfort (*TC*) and good air quality for occupants [2]. However, a recent study on *TC* showed that only 11% of 215 studied office buildings in United States, Canada and Finland equipped with HVAC systems were able to ensure comfortable states of the occupants [70]. The key to generating a suitable and effective indoor thermal environment for occupants is to correctly predict their *TC* state so that ventilation systems can perform corresponding adjustments to maintain acceptable comfort levels at times of operation [71]. Besides comfort, conventional HVAC systems consume high amounts of energy as they tend to condition the whole volume of the indoor space [4,28]. Thus, there is a great potential for significant reductions in energy consumption of HVAC systems to attain sustainability goals in indoor environments [2,4].

In moderate climates, natural ventilation (NV) is considered one of the most effective sustainable strategies for energy savings related to building usage while assuring the supply of adequate breathing air and acceptable ventilation of contaminants [11,12]. This makes NV a very attractive approach, nevertheless, the success of NV in providing *TC* for the occupants relies on the outdoor temperature and indoor loads. At the elevated indoor conditions above 26 °C which is the limit in typical office for acceptable comfort [53], attaining *TC* using NV as the only means of cooling would not be possible. Thus,

an additional system is required to maintain the occupants' TC , while consuming minimal energy. One of the most studied systems in the field of energy savings and comfort is personalized ventilation (PV) systems. PV units provide each occupant with the possibility to generate and control his/her own preferred microenvironment [7]. Several previous studies have integrated NV with PV and concluded that such integrated systems can save energy while still maintaining comfort levels of occupants [13, 14]. However, spaces conditioned by NV-PV systems are subjected to airflow and temperature transients causing variation in TC levels of the seated individual during hours of occupancy. Thus, the individual may have to perform recurrent and continuous changes to the operational settings of the PV (temperature and/or flow rate) to meet his/her comfort needs which is not practical as this affects working performance. For this reason, a dynamic NV-PV controller is needed to automatically adjust its settings whenever discomfort is detected while minimizing the intervention of the occupant.

The design of the dynamic PV controller primarily requires identification of the control parameters of the PV unit. In most of the PV operations, the occupant controls the flow rate while maintaining a constant PV supply temperature (T_{SPV}) [7,8,14,34]. Keeping T_{SPV} constant might fail in providing TC at elevated indoor temperature (T_{indoor}) as well as transients in T_{indoor} and relative humidity (RH) originating from NV [18]. Thus, changing both T_{SPV} and PV flow rate is important to avoid any possible discomfort condition. Moreover, TC should be maintained with transients that occur due to changes in the occupant's metabolic rate (activity level) from walking for example, before sitting at his/her desk. Allowing the occupant to simultaneously control the two PV supply variables might not bring the needed TC at the same rate versus when the person is

controlling a single operational variable. In fact, the authors are not aware of literature studies where the occupant is allowed to change the settings of two operational variables. In addition, the effect of changing a single variable can be quickly noticed by the occupant, such as changing the flow rate up to 15 L/s as adopted in many previous studies [14,33,7]. For example, at low T_{SPV} , the occupant might favor relatively low flow rate over the high flow rate while at high T_{SPV} , the occupant preference would be reversed. This direct relation between changing the supply flow rate and occupant TC at fixed T_{SPV} might become more complex and require from the occupant to juggle the PV operating conditions several times before a TC state is reached. Therefore, for NV spaces conditioned with PV, one variable, T_{SPV} , will be varied using a dynamic controller, while still allowing the occupant to change flow rate, if needed.

Estimating TC is critical for the success of the automated NV-PV system. Spaces conditioned by NV-PV systems bring failure of accurate TC prediction by means of conventional TC models such as PMV [1]. Thus, a model or correlation that can correctly predict TC in NV-PV spaces is needed. This correlation should predict TC when asymmetry, due to PV operation, in the environmental conditions surrounding the occupant exists. Since different individuals have different thermal sensations under the same environmental conditions [73], the correlation must rely on influential segmental physiological parameters to predict TC [71]. Physiological parameters, mainly segmental skin temperatures, were proven to be correlated with TC [74]. The body segments used in TC prediction should be of limited number and must not be covered to allow for the measurement of corresponding skin temperatures using non-invasive devices that do not affect the occupant's daily activities. Recent studies utilized thermographic cameras as

means to measure skin temperatures and then used them in TC modeling [4]. In a preliminary study of Burzo et al., average facial temperature was manually extracted using hand-held thermographic cameras and was used to predict subject's level of discomfort [19]. Pavlin et al. also used multiple forehead points, that showed minimum temperature deviation, as measure of TC . Ranjan et al. manually extracted head and hand temperatures from a thermographic camera to model the thermal needs of the space occupants [75]. These studies proved that average face temperature was highly correlated to TC and can be employed to predict the TC levels of occupants. Along with facial skin temperature, present research studies have suggested relating TC with indoor environmental parameters (T_{indoor} and RH) [72]. The TC correlation should be able to predict TC when transients in indoor conditions exist. Thus, combining environmental parameters as well as segmental skin temperatures of accessible body parts can help in developing a TC model that can correctly predict the comfort state of an occupant.

The current work aims to propose a method for developing a TC correlation that considers not only steady state but also transient comfort in a NV office space with PV, where typical temperature drifts and changes in metabolic rate exist. This correlation is important since it allows for TC prediction without having to do extensive or invasive measurements. Based on existing studies for predicting TC using noninvasive measurements, the main variables that could be adopted to predict TC under NV-PV system are proposed. These variables are associated with the indoor environmental conditions, physiological parameters of segmental skin temperatures and PV supply conditions under steady and transient states. Since people are not always stationary during

a typical working day from 9:00 AM to 18:00 PM, changes in the metabolic rate between 1 met (58 W/m²) and 2 met (116 W/m²) are considered.

There is a trend to move towards NV office buildings assisted with PV units to enhance sustainable cooling solutions, however, the viability of this option depends whether their combination (NV-PV) can provide *TC*. The developed *TC* correlation, applicable to steady and transient situations, is then utilized in developing dynamic controllers for NV-PV systems to provide *TC* at all times without occupants' intervention. Thus, a standalone PV unit, autonomously controlled to provide comfort, in a NV office space was developed, with T_{indoor} that ranges between 25 and 33 °C, and *RH* between 60 and 80%. The dynamic NV-PV controller is designed such that it robustly adjusts the T_{SPV} , at the occupant set flow rate, whenever an uncomfortable thermal state is detected. The controller sets the T_{SPV} based on the predicted *TC* from the developed regression equation. The proposed controller is implemented in a case study of an office space with moderate hot and humid indoor conditions that is within the constraints and applicability of the developed correlation. The transient profile of T_{indoor} and *RH* of the NV-office space [13] are determined using the building energy simulation software, IES-VE [41]. The developed dynamic controller is tested, and its performance is evaluated in terms of attaining *TC* by using direct simulations on the bioheat model of Al-Othmani et al. [44,39] and Zhang's *TC* model [18] for the tested case.

CHAPTER II

TC CORRELATION METHODOLOGY

The methodology for developing a versatile *TC* correlation is presented in the coming subsections. A brief description is provided on the different physical models used in the development of the correlation that include the bioheat model [39,44] and *TC* model (Zhang [18]). The range of indoor conditions and metabolic rates are identified for a NV-office space with local PV units during summer. The extensive simulated cases in these ranges for developing the correlation are presented including the correlation assessment method.

A. Methodology for developing the *TC* correlation and its influential variables

Fig. 1 shows a schematic of an office space that relies on NV, through open windows, and assisted with PV unit to provide *TC* for a seated occupant when NV indoor conditions are not sufficient to ensure occupants comfort. The occupant of NV-PV conditioned office experiences changes in thermal state due to transients induced by NV affected by changes in outdoor conditions and due to changes in occupant metabolic rate when activity level changes. This implies that environmental and space variables and physiological variables, along with their rate of change and PV operational settings need to be identified in order to develop a significant *TC* correlation. The proposed methodology for developing the correlation suitable for the NV-PV environment depends on several aspects summarized as follows:

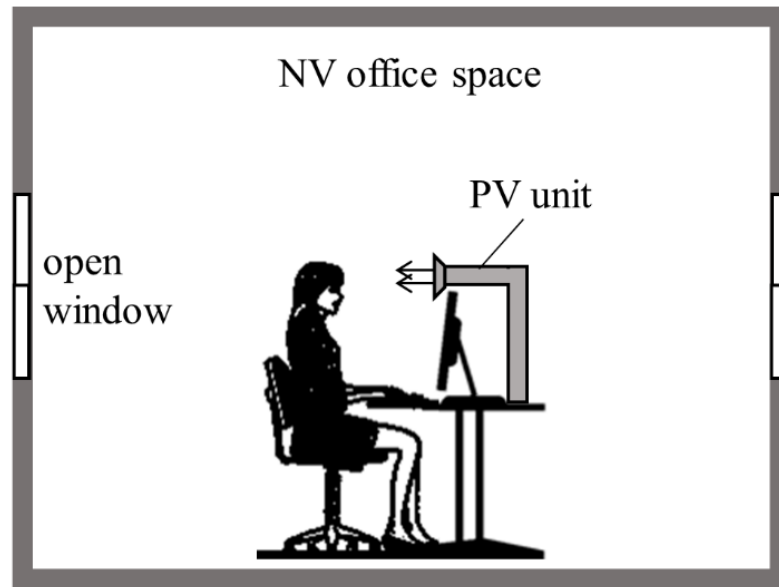


Fig. 1. Schematic of the NV-PV system in an office space

- 1) The availability of noninvasive measurements of skin temperature of exposed body segments and its rate of change are critical for the TC correlation. The facial and wrist skin temperatures and their rate of change (T_{facial} , T_{wrist} , dT_{facial}/dt and dT_{wrist}/dt) represent four possible physiological variables that can help in the development of the steady and unsteady comfort conditions. Since PV units supply treated fresh air towards the occupant's breathing zone [43,65,6], the exposed face would be an influential segment that could reflect the state of TC . Zhang reported that the face contributes significantly to improve TC when locally cooled with a whole body that is warm (Zhang 2003). Moreover, T_{wrist} was adopted in some previous TC measurement studies [18,19,66,67]. The importance of wrist temperature is assessed in the current study for a space equipped with a NV-PV system. The T_{facial} , T_{wrist} , dT_{facial}/dt and dT_{wrist}/dt can be easily measured using a noninvasive method

such as the thermal camera [20,57], and then can be related to the occupant *TC*. These variables are the most important data to be collected, independent of the location of the office space and the climatological data.

- 2) In a NV-office space, the following environmental and space variables are needed: T_{indoor} , dT_{indoor}/dt , and the indoor *RH*. Thus, the dependence of *TC* prediction on these parameters is examined under different indoor summer conditions.
- 3) Typical PV supply conditions adopted in literature ranged between 22 °C and 26 °C for T_{SPV} , and between 0 and 15 L/s for Q_{SPV} [8,9,22]. The dependence of *TC* prediction for different PV operational settings (Q_{SPV} and T_{SPV}) is studied, while assessing any interdependency that might be present with other variables such as T_{facial} , T_{wrist} , dT_{facial}/dt and dT_{wrist}/dt . It should be noted that the cases where T_{indoor} is equal to T_{SPV} are not considered.

To collect the proposed data (T_{facial} , T_{wrist} , dT_{facial}/dt , dT_{wrist}/dt , T_{indoor} , dT_{indoor}/dt , *RH*, T_{SPV} , and Q_{SPV}), the following models are used:

- i) IES-VE software applied for a NV office space [41] to predict T_{indoor} , dT_{indoor}/dt , and the indoor *RH*.
- ii) the validated segmental bioheat model [39,44] integrated with PV to predict physiological responses with or without local cooling; and
- iii) the actual *TC* votes collected using Zhang's comfort model [18], for the different indoor and PV supply conditions.

Moreover, multivariable linear regression was adopted in order to provide a simple tool for predicting *TC* with a hybrid cooling system using noninvasive measurements.

This method was previously used in other studies that involve a correlation development with several variables [61,62]. The facial and wrist skin temperatures and their rate of change along with the indoor conditions (T_{indoor} and RH) and PV operating conditions (Q_{SPV} and T_{SPV}) are the variables used in developing the TC correlation. The correlation is then evaluated with different case study scenarios, which included steady state conditions and realistic transient situations. The sources of transients are triggered by changes in the metabolic rate of the occupant that could be coming from a transition space at an elevated metabolic rate of 2 met and then sitting at his/her desk where the metabolic rate stabilizes at around 1 met. The proposed methodology for developing the TC correlation under NV-PV system is presented in **Fig. 2**.

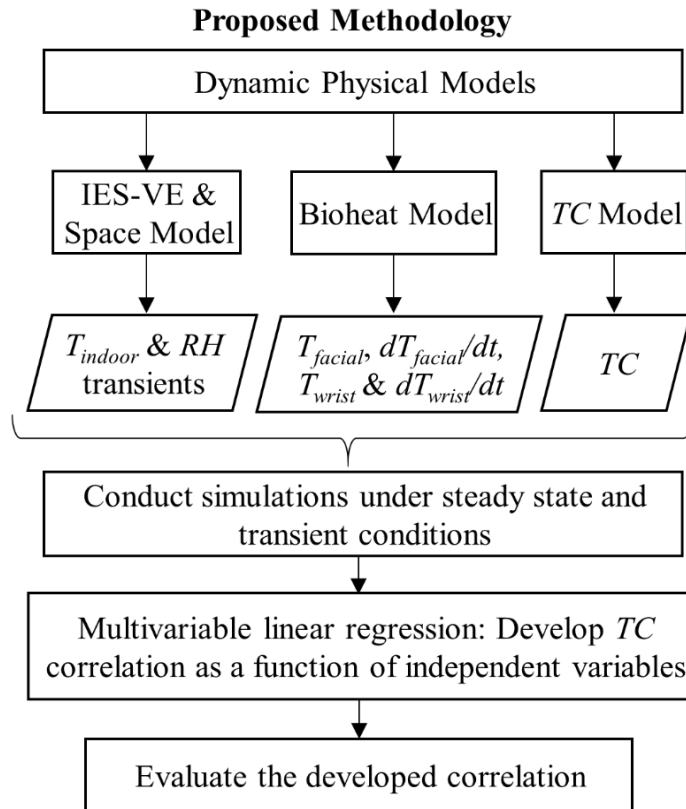


Fig. 2. Proposed methodology for developing a TC correlation under NV-PV system

B. The bioheat model

The segmental skin temperatures and the rate of change of 13 body segments (forehead, cheeks, backhead, chest, back, abdomen, upper arm, lower arm, palm, fingers, thigh, calf and foot) are predicted by a robust and previously validated bioheat model of Al-Othmani et al. [39]. **Fig. 3** shows a schematic of the multi-segmented human body with the main segments listed. The model has a relatively good accuracy when compared to published experimental data (maximum error in skin temperature prediction of ± 0.5 °C) [39,44,84]. Thus, this model can be used to predict T_{facial} (average temperature of the forehead and cheeks) and T_{wrist} , as the face and wrist are influential segments that can be targeted to predict TC [18]. The adopted bioheat model of Al-Othmani et al. [29] requires the following input data for conducting the simulations:

- Indoor conditions (T_{amb} , RH and air velocity) and exposure duration
- Metabolic rate that reflects the activity level
- Local convective coefficients that are affected by Q_{SPV} . When the PV is turned on, the convective heat transfer coefficients near the face, chest, and upper arms were computed according to the correlation of De Dear et al. [40] following the methodology of Al Assaad et al. [25].
- Clothing insulation and vapor diffusion characteristics of each body segment
- Physiological body data that include the basal metabolic rate, basal skin blood flow, minimum and maximum skin blood flow, sweating factor, cold shivering factor, surface area, and fat thickness of each body segment.

The outputs of the bioheat model that are relevant to the current study are basically the segmental skin temperatures corresponding to the 13 segments and their rate of change under transient conditions.

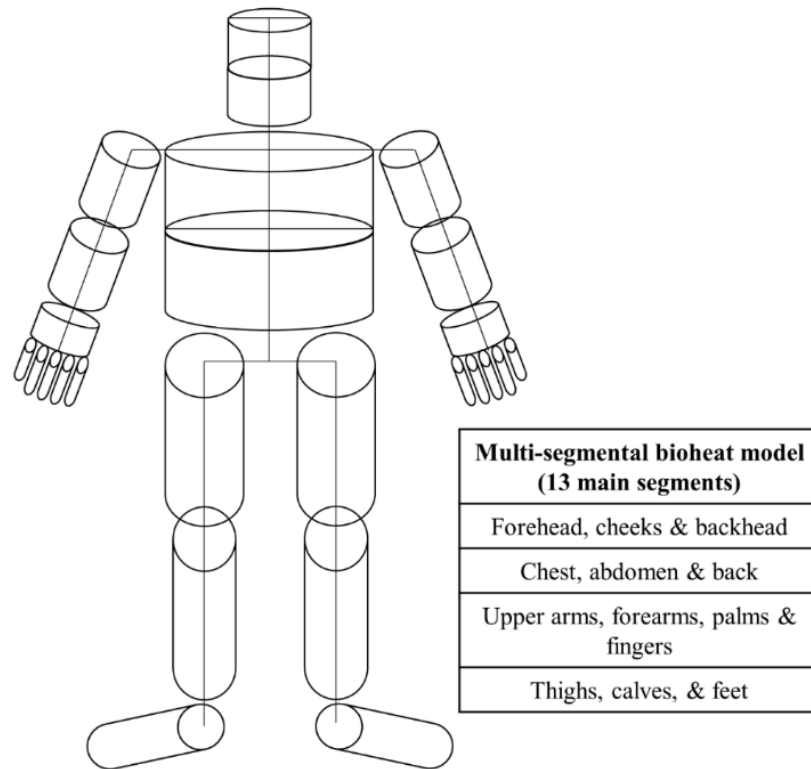


Fig. 3. Schematic of the multi-segmented human body as adopted in the bioheat model

C. Zhang (2003) *TC* model

The *TC* model of Zhang [18] was adopted in this study since it incorporates localized body cooling effects and effects of transients. The overall comfort model with localized cooling was based on experimental results of 109 human subjects involving 347 sets of data (skin and core temperatures and subjective votes) for steady state conditions and 3,568 data sets for transient conditions. Zhang's model (2003) predicts the local *TC* of the different body parts and then integrates the local *TC* in different proportion to form

the overall TC of the human body that varies on a scale ranging from **-4 (very uncomfortable) to +4 (very comfortable)** (Zhang 2003). Since the bioheat model [39,44] predicts the segmental core and skin temperatures and their rate of change, then local and overall TC could be easily evaluated using the model of Zhang (2003). Moreover, this model has been used in previous studies [25,36,26,27,13] since it can predict TC under transient and steady state thermal conditions as well as situations with individual control over the air supply conditions (2003).

D. The IES-VE NV office space model

The NV-office space adopted in this study has with medium weight concrete walls and is located in a moderately hot and humid climate as in Beirut, Lebanon [55, 85,13]. The space has typical internal loads during working hours and was calibrated by Khalil et al. [13]. It has a total area of 240 m² and is located in Beirut. It has windows on the four façades to allow for cross ventilation with a glazing percentage of 12% in the southwest and northeast façades, and 20% in the southeast and northwest façades. The existing windows are side-hung and can be opened to the outdoors at a maximum angle of 70°. All the previous information is needed as input to the IES-VE building energy simulation software [41] to predict T_{indoor} , dT_{indoor}/dt and RH . It should be noted that the cooling control strategy followed by Khalil et al. [13] is adjusted considering the windows to be fully opened during occupied hours without the aid of any mechanical cooling system. In addition, the adopted weather data are the Typical Meteorological Year estimated based on a period of 10 years extending from 2000 till 2009 [13]. Typical values of T_{indoor} range between 25 and 33 °C and RH between 55 and 80% [13,55,85]. The

obtained transients of T_{indoor} and RH , during the four summer months (June to September) from 9:00 AM to 18:00 PM, are summarized in **Table 1**.

Table 1: Typical T_{indoor} and RH during the four summer months

	June		July		August		September	
Time (hours)	T_{indoor} (°C)	RH (%)	T_{indoor} (°C)	RH (%)	T_{indoor} (°C)	RH (%)	T_{indoor} (°C)	RH (%)
9:00	25.1	68.0	26.1	74.6	27.3	62.0	25.1	59.0
10:00	26.9	65.5	28.1	69.4	29.2	60.8	27.1	56.2
11:00	28.2	63.9	29.2	65.4	30.5	59.3	28.4	54.5
12:00	29.0	63.1	30.0	62.7	31.3	57.4	29.2	53.8
13:00	30.3	63.2	31.2	61.4	32.5	56.2	30.5	54.2
14:00	30.8	64.1	31.8	61.3	33.0	56.4	31.1	55.5
15:00	30.2	65.8	31.2	62.5	32.5	59.8	30.5	58.0
16:00	29.4	68.3	30.5	65.0	31.5	63.0	29.4	61.4
17:00	27.7	71.7	28.5	68.9	29.8	69.3	27.7	65.9
18:00	27.1	75.9	28.1	74.0	29.5	70.3	27.4	71.4

E. Simulated cases for development of TC correlation

The proposed methodology for developing the TC correlation is applied to a NV-office space in a moderately hot and humid climate. The correlation should be also applicable to steady and transient situations. Thus, a total of 256 simulations were conducted using the bioheat and TC models [18,39,44] to develop the correlation under various possible summer indoor settings with steady state and transient conditions of metabolic rate, and transient conditions of T_{indoor} and RH . The simulations were conducted at different typical T_{SPV} and Q_{SPV} adopted in literature and reported as follows:

- T_{SPV} (°C) = [22, 24, 26]
- Q_{SPV} (L/s) = [0, 7, 10, 15]

It should be noted that at $T_{indoor} = 26$ °C, T_{SPV} at 26 °C is not considered in the simulation cases. The initial state of the human for the different simulations was found through the execution of the bioheat model for two hours to reach steady state in a preconditioned room. The clothing insulation adopted in the simulations is 0.57 clo (trousers, short-sleeve shirt, socks, shoes and underwear), which is typical in office spaces during summer [53]. In addition, the incorporation of the effect of PV was done through inputting the ambient temperature around the face to be equal to T_{SPV} and changing the corresponding heat transfer coefficient depending on Q_{SPV} , as stated in section II-B.

First, the steady simulations were conducted at typical average T_{indoor} and RH , during the morning (from 9:00 to 12:00 AM), mid-day (from 12:00 to 14:00 PM) and afternoon (from 14:00 to 18:00 PM) of the four summer months (June to September) [13,85] and summarized in **Table 2**. The steady simulations consider the occupant seated with a metabolic rate of 1 met. *A total of 114 steady simulations* were conducted:

- 12 simulations that consider an occupant seated at 1 met and at the 12 different morning, mid-day and afternoon indoor conditions of the four summer months listed in **Table 2** with PV turned off;
- 36 simulations at $T_{SPV} = 22$ °C at the 12 indoor conditions listed in **Table 2** and at the 3 different Q_{SPV} ;
- 36 simulations at $T_{SPV} = 24$ °C at the 12 indoor conditions listed in **Table 2** and at the 3 different Q_{SPV} ; and

- 30 simulations at $T_{SPV} = 26$ °C at the 10 indoor conditions listed in **Table 2** (excluding $T_{indoor} = 26$ °C) and at the 3 different Q_{SPV} .

Table 2: Typical average T_{indoor} and RH during the morning, mid-day and afternoon of the four summer months [13,85]

	Morning		Mid-day		Afternoon	
	T_{indoor} (°C)	RH (%)	T_{indoor} (°C)	RH (%)	T_{indoor} (°C)	RH (%)
June	26	65	30	63	27	71
July	27	70	31	62	28	71
August	29	60	33	59	31	68
September	26	56	30	55	28	64

Second, transient metabolic rate simulations (114 simulations) were conducted at the same indoor environmental conditions of **Table 2** and PV settings. However, the simulations consider an occupant that comes from a transition space at the same steady T_{indoor} and RH , but at an elevated metabolic rate of 2 met (walking at a speed of 3.2 km per hour) and then enters the NV-office space and sits for one hour in front of the PV unit with a gradual drop in the metabolic rate stabilizing at 1 met, as adopted by Zhu et al. [51]. The drop in the metabolic rate was implemented based on the equation of the oxygen uptake proposed by Barstow et al. [68]. The transient metabolic rate simulations did not consider simultaneous transients in the indoor conditions. This is due to the fact that the effect of the metabolic rate change on physiological responses only takes about 10 to 15 min to cease [51], while the effect of a typical change in T_{indoor} during this period of time is not as significant (see **Table 1**).

Finally, simulations considering transient conditions of T_{indoor} and RH were conducted, mimicking a NV office space with an occupant at fixed metabolic rate of 1 met during the whole working day from 8:00 AM to 5:00 PM. The adopted transients in T_{indoor} and RH of the four summer months (June to September) are summarized in **Table 1**. A total of 28 indoor transient simulations were conducted at the 4 summer indoor conditions listed in **Table 1**:

- 4 simulations with PV turned off;
- 12 simulations at $T_{SPV} = 22\text{ }^{\circ}\text{C}$ and the 3 different Q_{SPV} ; and
- 12 simulations at $T_{SPV} = 24\text{ }^{\circ}\text{C}$ and the 3 different Q_{SPV} . It should be noted that $T_{SPV} = 26\text{ }^{\circ}\text{C}$ was not considered since T_{indoor} goes below 26 during some of the months (see **Table 1**).

The values of instantaneous dT_{facial}/dt , dT_{wrist}/dt , dT_{indoor}/dt , and TC were found every minute for the transient metabolic rate and indoor simulations. Thus, the results of the conducted simulations are: *114 data points* for the steady simulations, $114\text{ simulations} \times 60\text{ minutes} = 6840\text{ data points}$ for the metabolic rate transient simulations, and $28\text{ simulations} \times 9\text{ working hours} \times 60\text{ minutes} = 15120\text{ data points}$ for the transient indoor conditions simulations.

F. Development and assessment of TC correlation

The correlation to predict TC was established as a function of noninvasively measured variables (T_{facial} , T_{wrist} , dT_{facial}/dt , dT_{wrist}/dt , T_{indoor} , dT_{indoor}/dt , RH , T_{SPV} , and Q_{SPV}) based on a set of simulations (using 22074 observations or data points) that mimic different real indoor scenarios, using multivariable linear regression. Multivariable linear regression was adopted in order to provide a simple tool for predicting TC with a cooling system that is hybrid with several variables that affect the prediction of TC . Thus, the general form of the developed correlation is shown in Eq. (1) for steady and transient conditions.

$$TC = \alpha + \beta_1 \times T_{indoor} + \beta_2 \times RH + \beta_3 \times T_{SPV} + \beta_4 \times Q_{SPV} + \beta_5 \times T_{facial} + \beta_6 \times T_{wrist} + \beta_7 \times \frac{dT_{indoor}}{dt} + \beta_8 \times \frac{dT_{facial}}{dt} + \beta_9 \times \frac{dT_{wrist}}{dt} \quad (1)$$

where α is the intercept of the line and $\beta_1, \beta_2, \beta_3, \beta_4, \beta_5, \beta_6, \beta_7, \beta_8$ and β_9 are the linear slope coefficients.

It is necessary to assess the developed correlation and to check the multicollinearity of the variables in order to establish a reliable and significant fitness function [59,60,61, 62]. A high degree correlation between the dependent variable, TC , and the independent variables is desired, while a low degree correlation between the independent variables is needed. Moreover, results of the ANOVA test should yield a value of the significance $F < F_{critical}$, in order to avoid having a high probability of a wrong regression equation. Finally, the significance of each one of the coefficients corresponding to the independent variables was tested and should yield a p -value < 0.05 .

CHAPTER III

NV-PV CONTROLLER METHODOLOGY

The methodology for developing a dynamic NV-PV controller is presented in the following subsections. Since the PV controller depends primarily on changing T_{SPV} to attain the target TC , there is a need to check whether the developed TC correlation is sensitive to any change in T_{SPV} . The applicability of the correlation is checked by using the bioheat and Zhang's TC models with a scenario of an initially uncomfortable seated person subjected to changes in T_{SPV} .

The developed control strategy for controlling T_{SPV} is then presented adopting a typical temperature proportional-integral-derivative (PID) controller. The followed methodology is presented for the design of the PID controller in terms of selecting its control parameters. The developed controller with its design parameters is finally implemented in a test case of a naturally ventilated office space. The indoor conditions are predicted using IES-VE software with proper internal loads and external ambient conditions specified, as shown in the flowchart for the developed methodology in **Fig. 4**. These indoor conditions need to be in the range of applicability of the selected TC correlation. The PV flow rate that the occupant can control varies between 7 L/s and 15 L/s, as commonly used in previous studies [8,9,22], while the range of T_{SPV} that can be set by the controller is between 22 °C and 26 °C [22,52]. To make sure that the NV-PV controller is working well, the bioheat and Zhang's TC models are needed to compare actual TC values with those predicted.

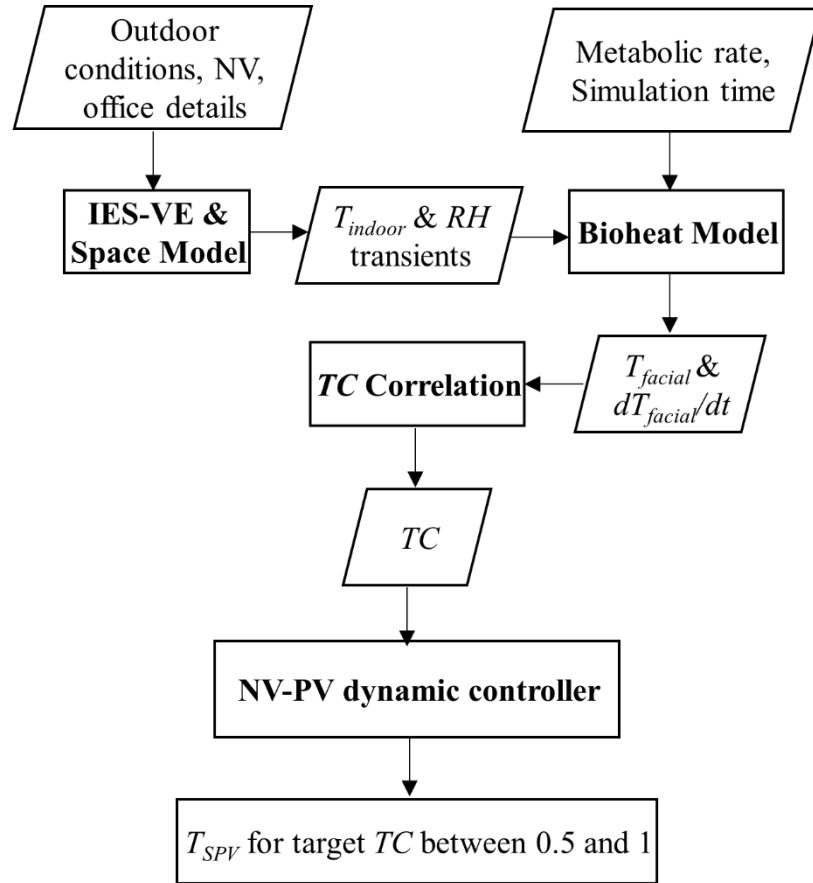


Fig. 4. Flow chart of the developed methodology

A. Applicability of the developed TC correlation

The success of the NV-PV controller depends on the ability of the TC correlation to predict the transient TC triggered by changing the T_{SPV} . There is a need to check for the sensitivity of the developed TC correlation [76] to changes in T_{SPV} . To this end, the accuracy of the TC correlation will be compared with the Bioheat-comfort predictor. A situation is considered of a person with a metabolic rate of 1 met in indoor conditions of $T_{indoor} = 30$ °C and $RH = 65$ % (within the applicability range of the TC correlation). The resultant TC status is not comfortable. In order to attain TC , the PV needs to be operated at T_{SPV} of 24 °C with a flow rate of 10 L/s. For a fixed flow rate, the PV is initiated at its

minimum allowed temperature of 22 °C to cause a significant improvement in TC . Then, T_{SPV} is increased gradually with an increment of 1 °C every 10 minutes, reaching its target value of 24 °C after which it is maintained constant for 40 minutes, as shown **Fig. 5**.

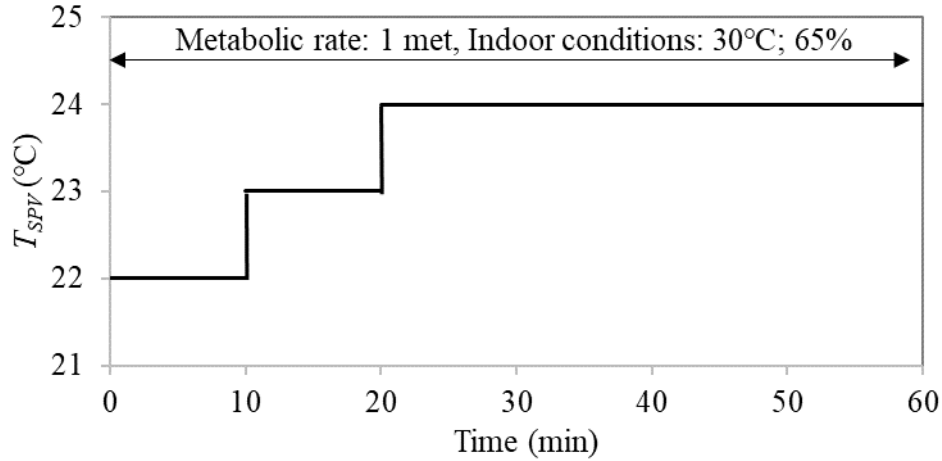


Fig. 5. Transient T_{SPV} profile under uniform indoor conditions

B. NV-PV dynamic controller

The temperature PID controller adopted in this study and the methodology followed for its parameter adjustments is described in subsection I. The NV-PV dynamic control strategy which utilizes the developed TC correlation in controlling T_{SPV} is then presented in subsection II.

I. PID controller and its parameter adjustment

In this work, a robust and high accuracy temperature controller is needed to first compare the current T_{SPV} with the required control set-point and then to provide the output to a control element. Since proportional-integral-derivative (PID) controllers employ

closed-loop feedback to keep the output as close as possible to a target or set-point value, it can be utilized in controlling T_{SPV} . Moreover, PID controllers react quickly to disturbances and give accurate set point temperature control [69,79]. In fact, PID controllers have been extensively used for temperature regulation and control due to its simple structure, easy implementation and strong robustness [79].

The PID controller runs for a total number of iterations, N . At each iteration of the algorithm $k \in [0, \dots, N]$, the PID reads the feedback value of present T_{SPV} , $(T_{SPV})_k$, and computes the difference between $(T_{SPV})_k$ and set PV temperature, $T_{SPV-set}$, as shown in **Fig. 6**. This difference is called the proportional error, E_k . The PID also computes the derivative error which is the difference between the proportional errors at iterations k and $k - 1$, notably $(E_k - E_{k-1})$. The last error computed by the PID is the integral error which is the sum of all temperature difference from the first iteration of the algorithm until the k^{th} iteration, i.e. $\sum_{t=0}^k E_t$. Each of the aforementioned errors is weighted by a gain, denoted by K_p, K_d and K_i for proportional, derivative and integral gain respectively. The weighted sum of these errors is then used by the PID and the PV system process to adjust T_{SPV} for the following iteration, $(T_{SPV})_{k+1}$. The PID algorithm keeps on reading the feedback value $(T_{SPV})_k$ and adjusting $(T_{SPV})_{k+1}$ as long as the difference between $T_{SPV-set}$ and $(T_{SPV})_k$ is higher than a given tolerance. The present temperature T_{SPV} can rapidly reach $T_{SPV-set}$ and be steadily kept constant as long as TC is not violated.

K_p, K_i , and K_d are the main control parameters of the PID controller and the correct determination of their values is the key design of temperature control systems. Since such are usually typical lag inertial systems, the manual trial and error method can be employed to determine the design control parameters [69]. To determine the proportional factor K_p ,

K_i and K_d are first set to zero. K_p is recorded once system oscillation is observed followed by a steady state convergence to $T_{SPV-set}$. In the practical application of PID, K_p should be 60 %-70 % of this recorded value [69]. After that, ki is increased until any offset is corrected in enough time for the process and is recorded. However, ki should be decreased slightly to avoid instability. Finally, K_d is increased until the loop is acceptably quick to reach its reference after a load disturbance with a notable decrease in overshoot. This tuning procedure is performed on a certain case under specific indoor and PV conditions presented in chapter V. The resulting gains of this case were then tested on several other cases, considering steady and transient indoor conditions, within the range of application and induced the best performance.

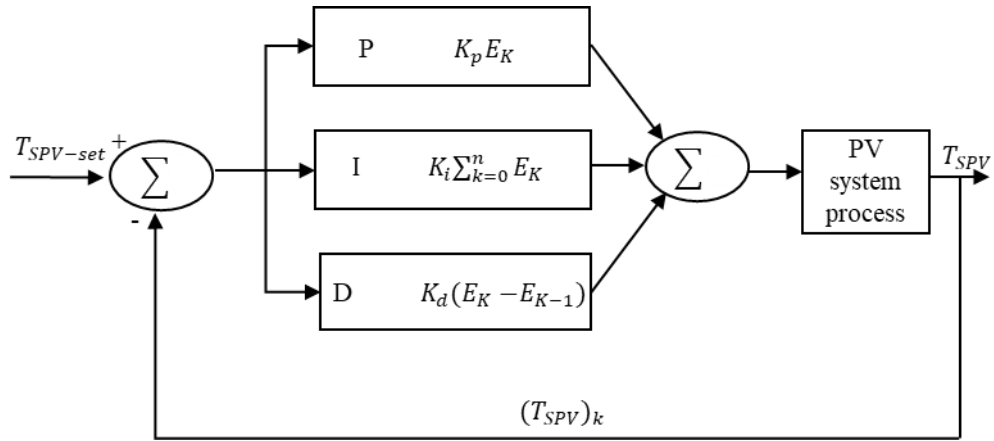


Fig. 6. NV-PV dynamic PID controller

II. NV-PV control strategy

The automated NV-PV dynamic controller changes T_{SPV} to meet target TC level. The PV can operate at a range of supply flow rates between 7 L/s and 15 L/s and supply temperatures between 22 °C and 26 °C [8,9,22]. The controller computes TC each minute

according to the developed TC correlation [79] and adjusts T_{SPV} , at the set flow rate, whenever an uncomfortable state is detected as shown in **Fig. 7**. A detailed control strategy of the PV controller is represented as follows:

- Four input parameters are measured each minute: T_{facial} , dT_{facial}/dt , T_{indoor} , and indoor RH .
- TC is predicted using the developed mathematical correlation
- If the predicted TC falls between the acceptable range of 0.5 and 1, T_{SPV} is not to change, otherwise a target T_{facial} , $T_{facial-set}$, that ensures a TC of 1 is calculated using the developed TC correlation
- The controller initiates the PV operation at a T_{SPV} of 22 °C and then adjusts it as desired according to the difference between the present T_{facial} and the target one, $T_{facial-set}$.
- If the difference is positive, T_{facial} should be decreased to reach the target value and thus T_{SPV} should be decreased too, otherwise T_{SPV} should be increased, given that T_{SPV} is bounded between 22 °C and 26 °C.
- The rate of change of T_{SPV} is deduced from bioheat simulations that show the effect of a one-degree Celsius change in T_{SPV} on T_{facial} . The rate of change of T_{SPV} was approximated to be proportional to the difference between required T_{facial} and present one. Thus, for every 0.3 °C facial temperature difference there should be a 1 °C change in T_{SPV} . The success of the adopted rate of T_{SPV} change was tested and validated with two cases shown in **Appendix A**.

- Conducted simulations on the bioheat model showed that a minimum change of $1\text{ }^{\circ}\text{C}$ in T_{SPV} is needed to induce a significant change in TC . Thus, the PID controller computes T_{SPV} and takes action once the increment/decrement in T_{SPV} is not less than $1\text{ }^{\circ}\text{C}$. The T_{SPV} can be varied every minute assuming a system response similar to that reported in previous studies [82,83].

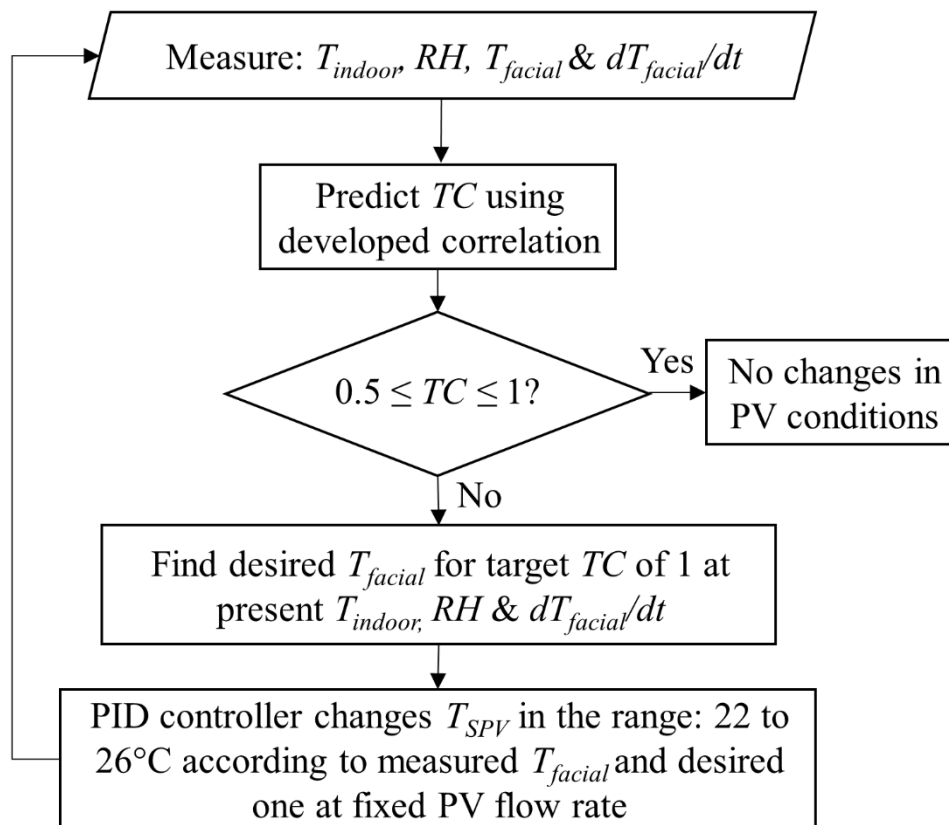


Fig. 7. NV-PV dynamic controller flowchart

CHAPTER IV

TC CORRELATION RESULTS

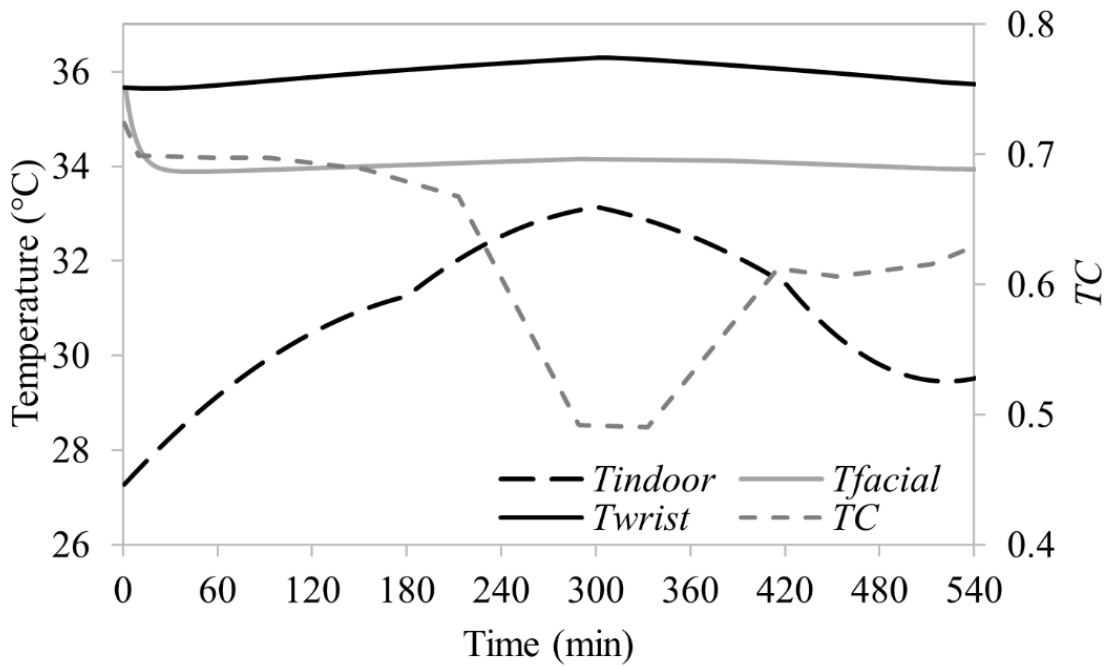
A sample of the actual data collected for developing the TC correlation is first presented. Then, the developed correlation for predicting TC is discussed, followed by its evaluation through comparison of predicted and actual TC applied to different cases studies. Finally, benchmarking with some experimental data was done and the main applications and limitations of the developed correlation are presented.

A. Sample of actual data collected for TC correlation development

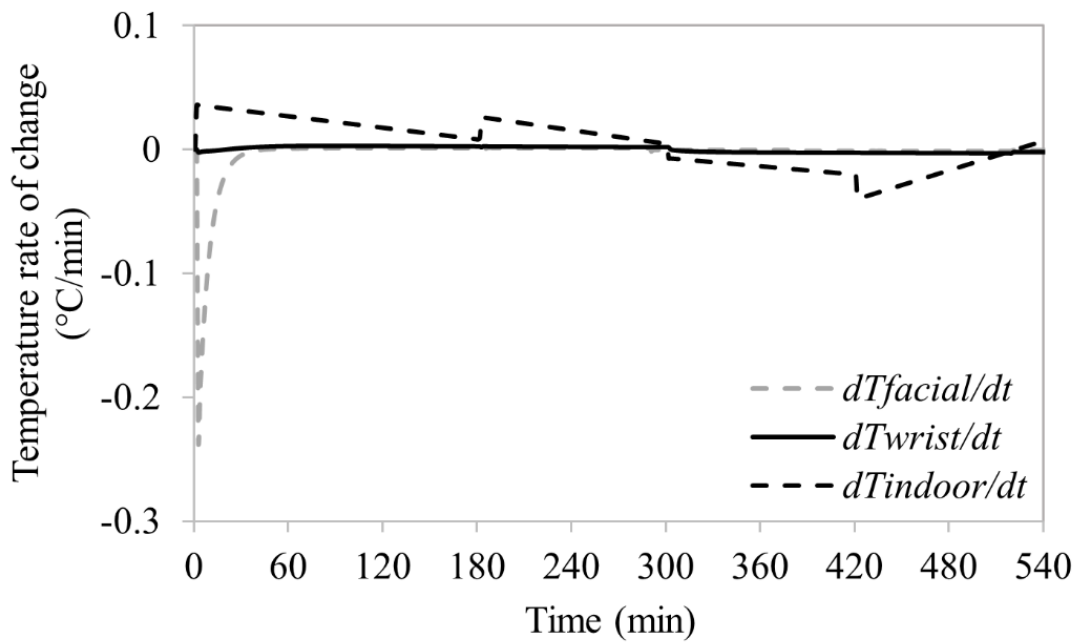
Results of the 256 conducted simulations (T_{facial} , T_{wrist} , T_{indoor} , RH , dT_{facial}/dt , dT_{wrist}/dt , dT_{indoor}/dt and actual TC) were collected in order to develop the TC correlation. A sample of these data for a case that considers an occupant seated at a constant metabolic rate of 1 met during the working hours of August (variable indoor conditions shown in **Table 1**) with $T_{SPV} = 22$ °C and $Q_{SPV} = 10$ L/s turned on at the start of the working day, is presented in **Fig. 8**. Transient variation of T_{facial} , T_{wrist} , T_{indoor} , and TC are presented in **Fig. 8(a)**, while **Fig. 8(b)** shows the transient variation of dT_{facial}/dt , dT_{wrist}/dt , and dT_{indoor}/dt . Initially, T_{facial} and T_{wrist} start decreasing with a more significant drop in T_{facial} from 35.6 °C to 33.8 °C in the first 40 min due to the direct effect of the PV on the face. Thus, dT_{facial}/dt and dT_{wrist}/dt became negative with dT_{facial}/dt reaching a significant value of -0.23 °C/min, as shown in **Fig. 8(b)**. Meanwhile, T_{indoor} is increasing as shown in **Fig. 8(a)**, which means that dT_{indoor}/dt is a positive value during this time, as shown in **Fig. 8(b)**. During this time, TC was around 0.7 indicating a just comfortable state. After about 40

min, the effect of having the PV turned on was not enough to maintain the same TC state (dropped to 0.49 as shown in **Fig. 8(a)**) as T_{indoor} increased reaching 33.1 °C after 300 working minutes. Accordingly, T_{facial} and T_{wrist} had increasing trends but with low rates of change, as shown in **Fig. 8(b)**. After 300 min, T_{indoor} started decreasing reaching 29.5 °C at the end of the working day, which caused slight drops in T_{facial} and T_{wrist} , and consequently improvement in TC , as shown in **Fig. 8(a)**.

The actual data for another case are similarly presented in **Fig. 9**. This case considers an occupant, initially at a relatively high metabolic rate of 2 met, at $T_{indoor} = 29$ °C, and $RH = 60\%$ with the PV turned off, that sits in front of a PV unit with $T_{SPV} = 22$ °C and $Q_{SPV} = 15$ L/s for one hour and same indoor conditions, while the metabolic rate gradually drops to 1 met [68]. Initially, T_{facial} and T_{wrist} start decreasing with a more significant drop in T_{facial} from 35.7 °C to 33.6 °C in the first 25 min (see **Fig. 9(a)**), due to the direct effect of the PV on the face while the metabolic rate decreases from 2 met. Accordingly, dT_{facial}/dt and dT_{wrist}/dt were negative with dT_{facial}/dt reaching a significant value of -0.28 °C/min, as shown in **Fig. 9(b)**. As for TC , an overshoot was noticed in the first 2 min, as shown in **Fig. 9(a)**, followed by a gradual increase in TC as the metabolic rate decreased and PV kept on. After about 25 min, the transient variations of the different variables started reducing until steady values were reached in the last 20 min. TC , T_{facial} and T_{wrist} stabilized at 1.9 (comfortable), 33.55 °C, and 35.8°C, respectively, while dT_{facial}/dt and dT_{wrist}/dt became 0, as shown in **Fig. 9**.



(a)



(b)

Fig. 8. Sample of collected data of skin temperatures, indoor conditions and their rate of change under August indoor condition transients

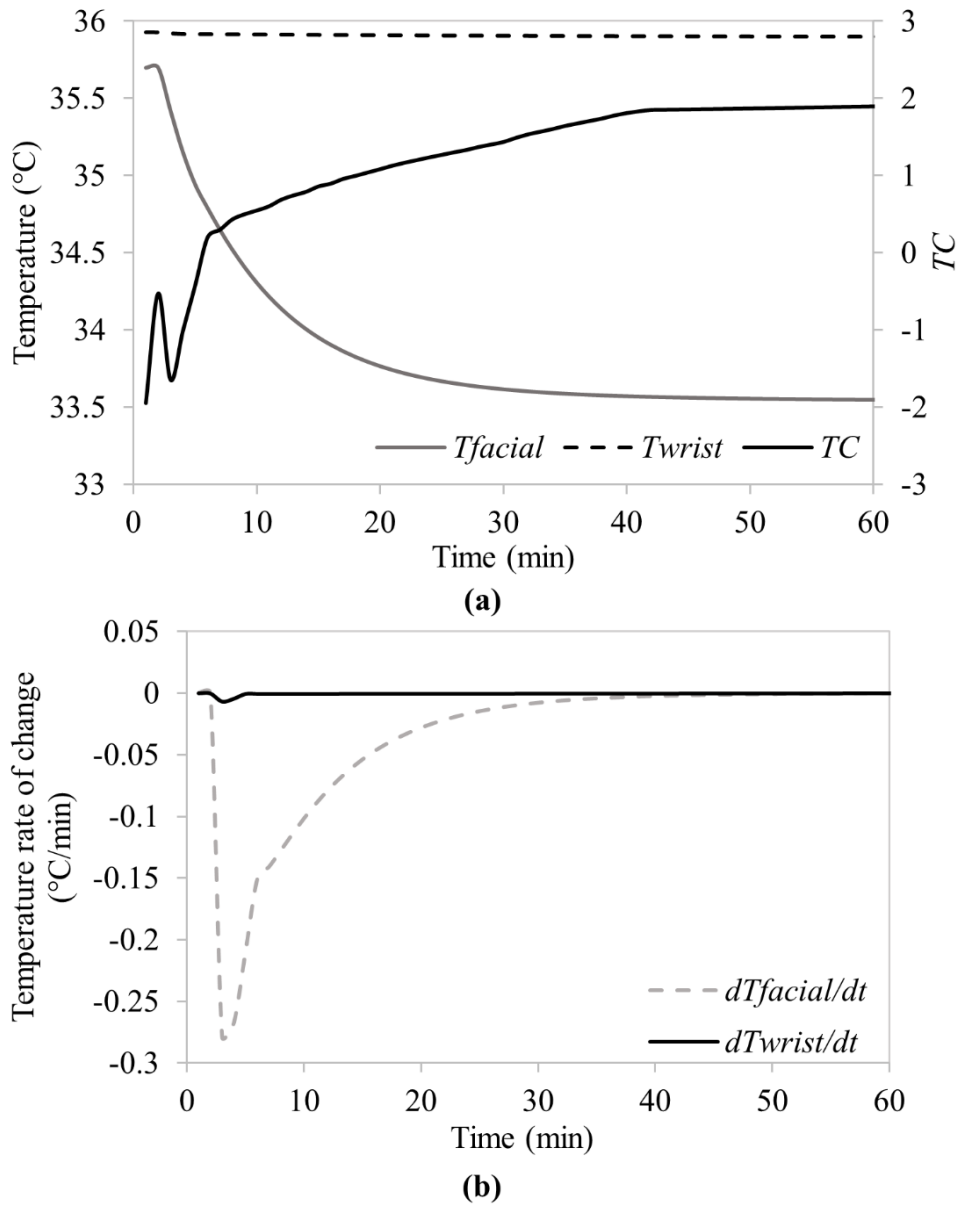


Fig. 9. Sample of collected data of skin temperatures, indoor conditions and their rate of change under metabolic rate transients

B. Multivariable linear regression analysis

After collecting all the data from the conducted simulations, assessment of the developed correlation was done through checking for any multicollinearity in the different variables (TC , T_{facial} , T_{wrist} , dT_{facial}/dt , dT_{wrist}/dt , T_{indoor} , dT_{indoor}/dt , RH , T_{SPV} , and

Q_{SPV}). In addition, the significance of each one of the coefficients corresponding to the independent variables was tested to eliminate variables with a p -value > 0.05 .

It was found that not all the variables were significantly correlated with TC . Mainly T_{wrist} , dT_{wrist}/dt , and dT_{indoor}/dt , were poorly correlated with TC (correlation < 0.2 and p -value > 0.05). As shown in **Fig. 8** and **Fig. 9**, T_{wrist} and dT_{wrist}/dt did not vary significantly to trigger a change in TC , either with indoor or metabolic rate transients and with PV operation. This could be attributed to the fact that with NV-PV system, the face is the main segment affected by the local cooling applied using the PV unit, and thus it is the major segment affecting TC and its transients. In addition, the transients in T_{indoor} were not significant (average maximum dT_{indoor}/dt of 1.2 °C per hour) to cause a substantial change in TC from the steady state value at the same T_{indoor} . Finally, the variables T_{SPV} and Q_{SPV} showed a high degree of correlation (correlation > 0.6) with the variable T_{facial} . This is a reasonable result, since any change in T_{SPV} and Q_{SPV} would directly affect the face skin temperature. Consequently, a regression equation that describes the relationship between the remaining independent variables, T_{indoor} , RH , T_{facial} and dT_{facial}/dt , and the dependent variable, TC , was obtained for NV-PV system and is defined in Eq. (2).

$$TC = -0.1365 \times T_{indoor}(\text{°C}) - 0.0012 \times RH(\%) - 1.0804 \times T_{facial}(\text{°C}) + 6.0248 \times \frac{dT_{facial}}{dt}(\text{°C}/\text{min}) + 41.9906 \quad (2)$$

Regression coefficients, also known as slope coefficients, represent the mean change in TC for one-unit change in the considered variable while maintaining other variables constant. The equation shows that the coefficients for T_{indoor} and RH are -0.1365 and -0.0012, respectively, meaning that for every additional degree Celsius in T_{indoor} or 1% in

RH , TC is expected to decrease by 0.1365 and 0.0012, respectively. This is anticipated since hotter and more humid conditions would decrease TC . In addition, T_{facial} has a significant impact on TC , as for each additional degree Celsius in T_{facial} a decrease in TC by 1.0804 is expected.

For transient situations, dT_{facial}/dt is considered very critical for TC evaluation. So, for every additional degree Celsius per minute in dT_{facial}/dt , TC is expected to increase by 6.0248. In other words, for an increase of 1 unit on the TC scale, dT_{facial}/dt has to change by 0.166 degree Celsius per minute. In fact, in the presence of PV, T_{facial} is decreasing and thus dT_{facial}/dt is negative but decreasing as well, while TC improves as desired. Regression statistics and ANOVA test of the final TC correlation variables have been conducted and the results are summarized in **Table 3**. The multivariable linear regression model demonstrated that the correlation was significant, with an adjusted R^2 value of 0.81. All the statistical results support that the developed correlation has good prediction capacity given that no multicollinearity was observed between the final variables in the correlation test.

Table 3: Regression Statistics and ANOVA

R^2	0.81
Adjusted R^2	0.81
Significance F	0.00
$F_{critical}$	2.37
p -value	< 0.05

C. *TC* correlation evaluation results

In this section, the evaluation results of the *TC* correlation are presented. The number of observations used as the training data for the linear regression equation was 22074, as discussed in section II-E. To check if the developed equation performs well, the predicted *TC* is compared against the actual *TC* as shown in **Fig. 10**. A strong linear relation between the actual and the predicted *TC* is depicted in **Fig. 10** with an R^2 value of 0.813, indicating that the developed equation can correctly predict *TC*. The regression analysis results showed that the standard error in predicting *TC* was 0.4 as shown in **Fig. 10**.

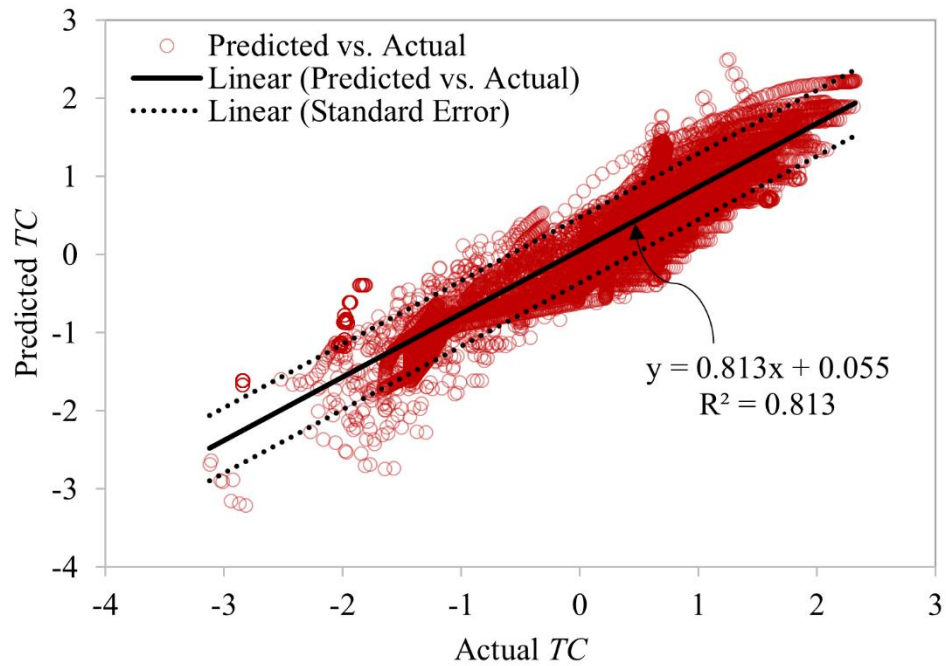


Fig. 10. Scatter plot for predicted versus actual *TC* corresponding to all the observations under steady and transient conditions

Data points, outside the data set or observations used in developing the correlation, were also used to evaluate the accuracy of the developed correlation under steady and transient conditions. These cases represent a seated occupant with a constant metabolic rate of 1 met in an office with constant T_{indoor} and RH . The results of the predicted versus

actual TC under steady state conditions are summarized in **Table 4**. For example, at $T_{indoor} = 27.50$ °C, $RH = 61\%$, and $T_{facial} = 34.71$ °C, the predicted TC was 0.66, which is in good agreement with the actual TC of 0.60.

Table 4: Evaluation of the TC correlation using 6 outside-data points representing steady state situations

Data no.	T_{indoor} (°C)	RH (%)	T_{facial} (°C)	TC actual	TC predicted
1	26.50	60	35.41	0.04	0.04
2	27.50	61	34.71	0.60	0.66
3	29.50	78	34.82	0.29	0.25
4	30.50	72	34.47	0.49	0.50
5	31.50	65	34.40	0.47	0.45
6	32.50	68	34.66	0.08	0.03

Under transient conditions of metabolic rate, three data sets from the observations used in developing the regression equation along with three data sets outside the observations were adopted to assess the accuracy of the TC equation. The observation cases were selected to show examples where the predicted TC was highly correlated with the actual one and an example with low correlation with actual. The transient cases considered a person who came from a transition space with a relatively high metabolic rate of 2 met and then entered an office space to sit for one hour, leading to a decrease in the metabolic rate reaching a final value of 1 met [68]. The three observation cases under consideration are:

- **Case A:** $T_{indoor} = 28$ °C, $RH = 64\%$, $T_{SPV} = 24$ °C and 7 L/s.
- **Case B:** $T_{indoor} = 30$ °C, $RH = 63\%$, $T_{SPV} = 26$ °C and 15 L/s.
- **Case C:** $T_{indoor} = 33$ °C, $RH = 59\%$, $T_{SPV} = 22$ °C and 10 L/s.

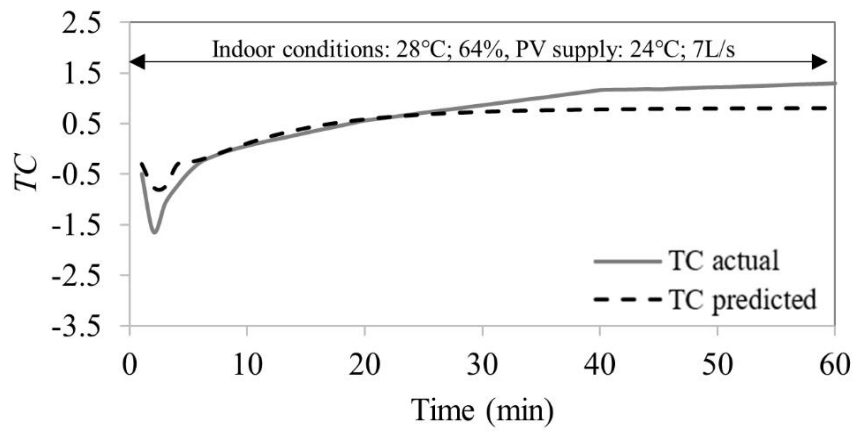
The three outside-data set cases under consideration are:

- **Case 1:** $T_{indoor} = 27.5$ °C, $RH = 65\%$, $T_{SPV} = 23$ °C and 12 L/s.
- **Case 2:** $T_{indoor} = 30.5$ °C, $RH = 68\%$, $T_{SPV} = 24$ °C and 13 L/s.
- **Case 3:** $T_{indoor} = 30.5$ °C, $RH = 62\%$, $T_{SPV} = 25$ °C and 8 L/s.

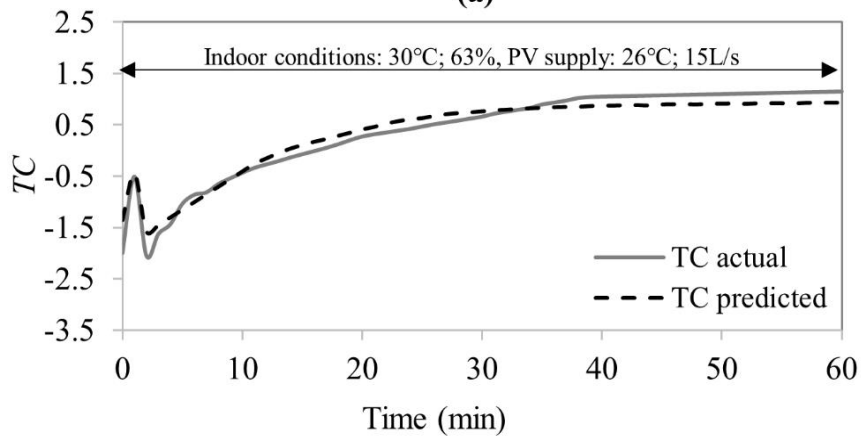
Fig. 11 shows the predicted and actual values of TC under transient conditions for (a) **Case A**, (b) **Case B**, and (c) **Case C** which are the observation cases. In all the considered cases, the occupant enters the office space at a high metabolic rate of 2 met feeling generally uncomfortable and then sat with a decreasing metabolic rate that reached 1 met with the PV unit turned on. Due to local cooling and the decrease in metabolic rate with the drop in oxygen uptake [68], actual TC improved quickly with an overshoot at the very beginning and then decreased followed by a gradual increase reaching a steady TC value about 1.3, 1.4 and 1.0 for **Case A**, **Case B** and **Case C**, respectively. This overshoot in TC was similarly reported by Jin et al. [86]. **Case A** is an example where the predicted TC was not well correlated with the actual one, and the maximum deviation in TC prediction was about 0.8 in the first 2 min. The predicted TC followed a similar trend compared to the actual TC but with a deviation in the first 2 minutes for **Case B** and **Case C**. The overshoot in TC was predicted by the developed model to an acceptable degree of accuracy compared to the actual TC . After the first 5 minutes, the deviation between predicted and actual TC decreases with a maximum difference of about 0.3 at the end of exposure time for **Case B** and **Case C**, which showed a highly correlated TC prediction.

Fig. 12 shows the predicted and actual values of TC under transient conditions for (a) **Case 1**, (b) **Case 2**, and (c) **Case 3** which are outside-data cases. Similar to previous discussion made on **Fig. 7**, the predicted TC followed a similar trend compared to the

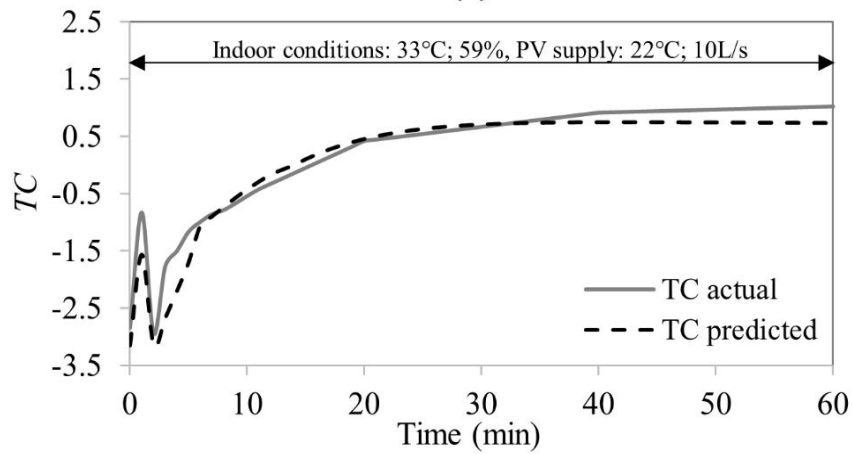
actual TC , with a maximum deviation of 0.5 in the first 5 minutes. After that, the deviation between predicted and actual TC decreased with a maximum difference of about 0.1 at the end of exposure time. The maximum deviation between predicted and actual TC for both the external data and the observation cases was about 0.5. In general, the results showed good agreement between the predicted and actual TC values. In addition, the TC regression equation was able to predict the transient variation in TC , as shown in the first few minutes with the drop in the metabolic rate and PV operation.



(a)



(b)



(c)

Fig. 11. Comparison between the predicted and actual TC values under transient conditions of metabolic rate for 3 observations: (a) **Case A**, (b) **Case B**, and (c) **Case C**

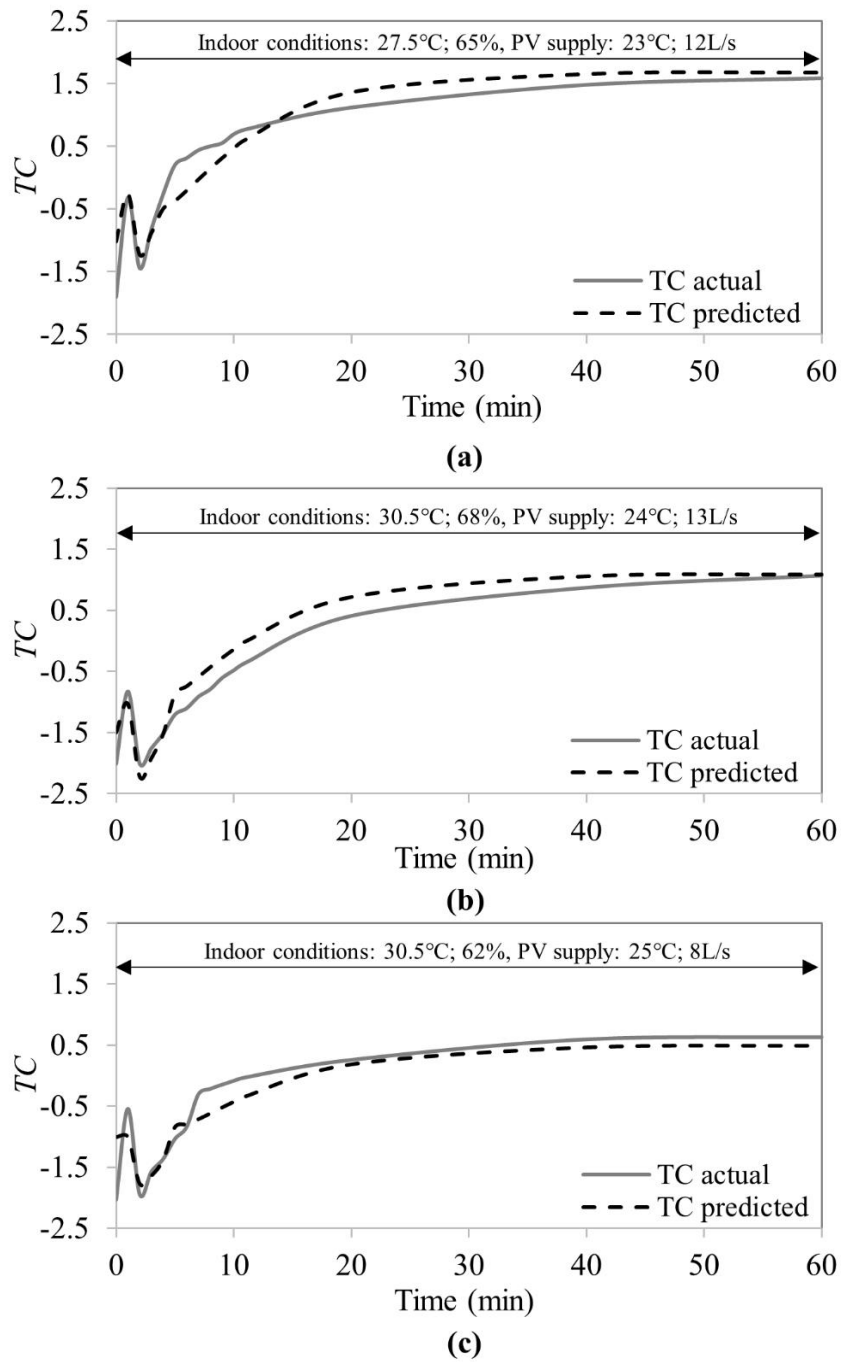


Fig. 12. Comparison between the predicted and actual TC values under transient conditions of metabolic rate for 3 outside-data sets: (a) **Case 1**, (b) **Case 2**, and (c) **Case**

The literature studies that focused on predicting personal TC from noninvasive measurements of T_{facial} and T_{indoor} did not report a simple TC correlation as they lacked enough experimental data on human subjects to be able to develop a generalized model. In addition, there is no standard method that could be used to perform the comparison between the different studies [1,71]. Consequently, benchmarking was conducted to compare the predicted TC using the developed correlation with experimental data reported in literature for steady conditions without local face cooling of Pavlin et al. [75] and for transient conditions with local face cooling of Zhang [18].

Pavlin et al. [71] exposed human subjects to transient variation of T_{indoor} between 21°C and 27°C with $RH = 50\%$ and no local cooling applied, until steady state conditions were attained at 21 and 27°C for forehead skin temperature, TC and thermal sensation. **Table 5** shows the comparison results between predicted and actual experimental data for TC . At $T_{indoor} = 21$ °C, the reported thermal sensation was close to neutral with forehead temperature of 34.3 °C, while at $T_{indoor} = 27$ °C it was a slightly warm sensation with forehead temperature of 36 °C. Accordingly, plugging these inputs into the developed TC correlation with $dT_{facial}/dt = 0$, predicted a TC of about 2 at 21 °C (comfortable state) and a TC of about -0.66 at 27 °C (slightly uncomfortable). The results show that the developed correlation can reflect the thermal state of the occupant when PV units are turned off at steady state conditions.

Zhang [18] conducted a transient experiment that included face cooling with an air temperature of 23 °C at $T_{indoor} = 28$ °C and $RH = 50\%$ (assumed). The initial reported steady state T_{facial} and TC were 36.0 °C and -0.9 (slightly uncomfortable), respectively,

which improved to 32.0 and 1.3 (slightly comfortable), respectively, after applying face cooling with dT_{facial}/dt of -0.4 °C/min (see **Table 5**). The initial predicted TC was -0.8 (slightly uncomfortable), which improved to 1.1 (slightly comfortable) after applying the face cooling. Thus, the predicted TC is in good agreement with the experimental reported data.

Table 5: Benchmark of results for the TC correlation

Reference	T_{indoor} (°C)	RH (%)	T_{facial} (°C)	dT_{facial}/dt (°C/min)	TC actual or thermal sensation	TC predicted
Pavlin et al. (2017)	21	50	34.3	0.0	thermal sensation close to neutral	2.00 (comfortable state)
Pavlin et al. (2017)	27	50	36.0	0.0	slightly warm sensation	-0.66 (slightly uncomfortable).
Zhang (2003)	28	50	36.0	0.0	-0.90 (slightly uncomfortable)	-0.80 (slightly uncomfortable)
Zhang (2003)	28	50	32.0	-0.4	1.30 (slightly comfortable)	1.10 (slightly comfortable)

CHAPTER V

NV-PV CONTROLLER RESULTS

The applicability of the developed TC correlation to the NV-PV system is first examined by checking the effect of transient changes in T_{SPV} on predicted TC . Then, the PID control parameters are selected based on the manual trial and error method. Finally, the performance of NV-PV controller is evaluated, in a case study scenario, based on its success in maintaining the target TC level.

A. Effect of transient changes in T_{SPV} on TC results

The applicability of the developed TC correlation to the design of the system is examined by analyzing the results of the scenario presented in section II-B. After collecting T_{facial} from the conducted simulation, TC is predicted using the developed TC correlation and compared to the actual comfort from Zhang's TC model [18] as plotted in **Fig. 13**. Under the uniform indoor conditions of $T_{indoor} = 30$ °C and $RH = 65$ %, a seated occupant would generally feel uncomfortable with predicted TC of -1.2. During the first 10 minutes, a T_{SPV} of 22 °C caused a further drop in TC to -2.6 due to the overcooling effect after which TC starts to increase reaching -0.06. When T_{SPV} is increased to 23 °C, predicted TC had a slight overshoot as shown in **Fig. 13**, which is similar to what happened with the actual TC level. T_{SPV} remained at 23 °C for the next 10 minutes and TC improved reaching 0.6, which is an acceptable TC level. Finally, for the last 40 minutes of operation, a T_{SPV} of 24 °C succeeded in maintaining TC between 0.5 and 1. The predicted TC followed a similar trend compared to the actual TC with an average

deviation of 0.1. The results show that the developed TC correlation can be used in the design of the dynamic controller as TC is proven to be sensitive to changes in T_{SPV} .

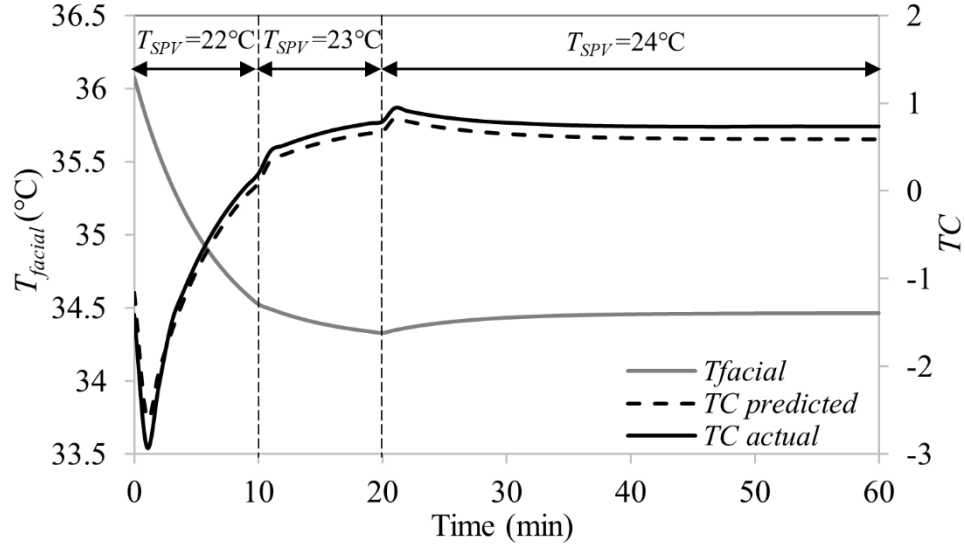


Fig. 13. Effects of transient changes in T_{SPV} on T_{facial} and TC .

B. PID control parameters using trial and error

The three main control parameters of the PID controller are the K_p , K_i , and K_d and are determined using the manual method of trial and error. This method was adopted for a specific case under the indoor and PV conditions presented in **Table 6**. At the considered conditions, T_{SPV} of 22 °C caused an increase in predicted TC above the target range. Therefore, to maintain a TC between 0.5 and 1, T_{facial} is to be slightly increased to a $T_{facial-set}$ of 34.45 °C. Accordingly, the target set value, $T_{SPV-set}$, is computed to be 23°C. The PV system process should therefore increase T_{SPV} from 22 °C to 23 °C. **Fig. 14** shows the output T_{SPV} after 60 iterations. The PID with K_p , K_i , K_d set to 0.2, 0.2 and 0.5 respectively gave the fastest response with the least overshoot compared to the other 2 cases. However,

in the practical application of PID, K_p , K_i , K_d can be set to 0.12, 0.18 and 0.5 respectively to avoid instability as previously discussed in section III-B-I.

Table 6: Indoor space and PV conditions to tune the PID controller

T_{indoor} (°C)	RH (%)	T_{SPV} (°C)	T_{facial} (°C)	TC predicted	$T_{facial-set}$ (°C)	$T_{SPV-set}$ (°C)
27	71	22	34.18	1.29	34.45	23

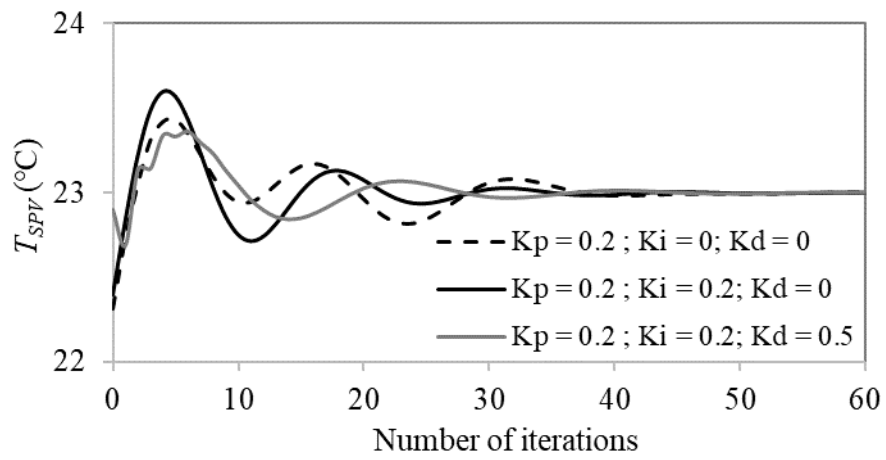


Fig. 14. Tuning PID controller for a specific case

CHAPTER VI

CASE STUDY

A. Case study for real-time implementation and testing of NV-PV dynamic controller

The space considered in this study is a typical office building with typical internal loads during the summer season. The calibrated office space developed by Khalil et al. [13], as shown in **Fig. 15**, was adopted in this study. The office space was located in Beirut, Lebanon, with a total area of 240 m². The weather data are the Typical Meteorological Year (TMY) data estimated based on a period of 10 years extending from 2000 till 2009 [13]. The cooling control strategy followed in Khalil et al.'s work [13] was adjusted considering the windows to be fully opened during the occupied hours without the aid of any mechanical cooling system.

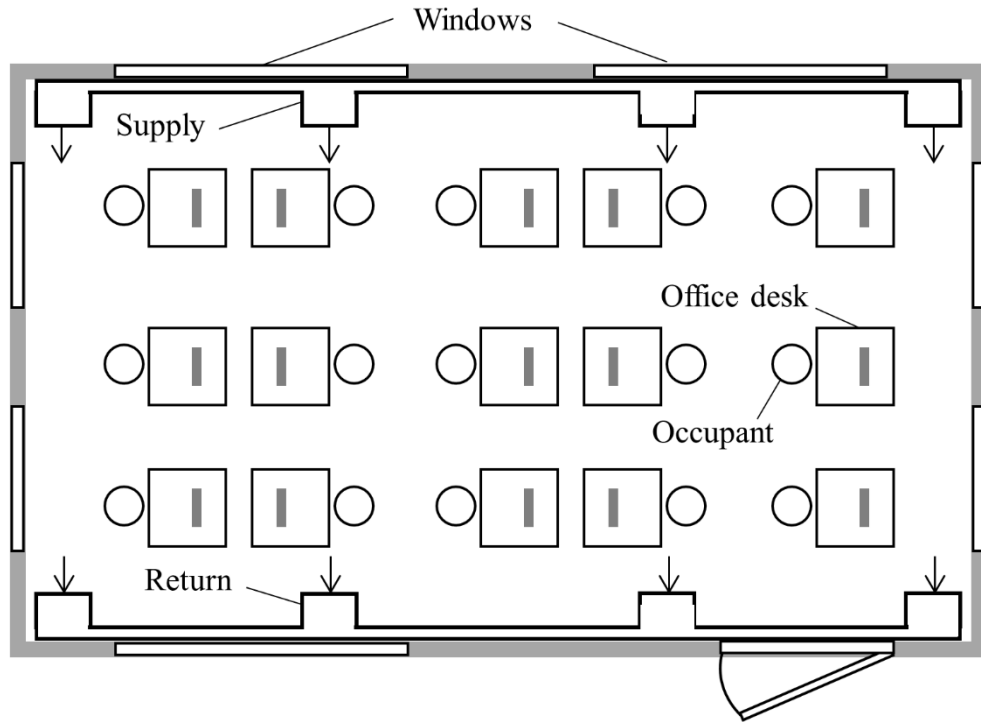


Fig. 15. Schematic showing the plan view of the simulated office space

A simulation case study scenario that resemble real situation was conducted to test the dynamic response of the NV-PV controller and its ability to maintain TC at its target value on the bioheat model. The case study considers transients in indoor conditions over a typical working schedule, along with transients in the metabolic rate of a person arriving at 9 AM at the office and leaving for a one-hour break at noon, to return to the office and leave it at 6 PM. The adopted transient profile in the metabolic rate over the working hours is shown in **Table 7**. A simulation is done using IES-VE to find the transient indoor conditions (T_{indoor} and RH) for the representative day of August, which is a typical hot and humid summer month. These indoor conditions as well as the metabolic rate profile are needed as input to the bioheat model to predict the actual T_{facial} and its rate of change. These variables (T_{indoor} and RH , T_{facial} and its rate of change) are used as inputs to the

controller that would recommend T_{SPV} over the simulated time. The target value of TC based on the recommended T_{SPV} should be between 0.5 and 1 during all the simulation period to assure good testing results of the controller.

Table 7: Metabolic rate profile over the working hours adopted in each of the case studies

Time (hr)	Metabolic rate profile
9 A.M.	Metabolic rate drops from 2 met at the end of the preconditioning period to stabilize at 1 met after occupant gets seated
12 noon	Occupant leaves the office to a break at metabolic rate of 1 met
12-1 P.M.	Occupant is exposed to the same transient T_{indoor} and RH but at elevated metabolic rate of 2 met
1 P.M.	Metabolic rate drops from 2 met at the end of the break period to stabilize at 1 met after occupant gets seated

B. Case study evaluation results

Simulation of the study case scenario was conducted to test the dynamic response of the NV-PV controller and its success in maintaining a target TC between 0.5 and 1. The transient indoor conditions (T_{indoor} and RH) for the representative day of August are shown in **Fig. 16** as outputted from the IES-VE software. The time variation in T_{SPV} as recommended by the NV-PV controller and the corresponding T_{facial} are presented for a

typical working day of the month of August in **Fig 17(a)**. In addition, a comparison between the predicted and actual TC are illustrated in **Fig. 17(b)**.

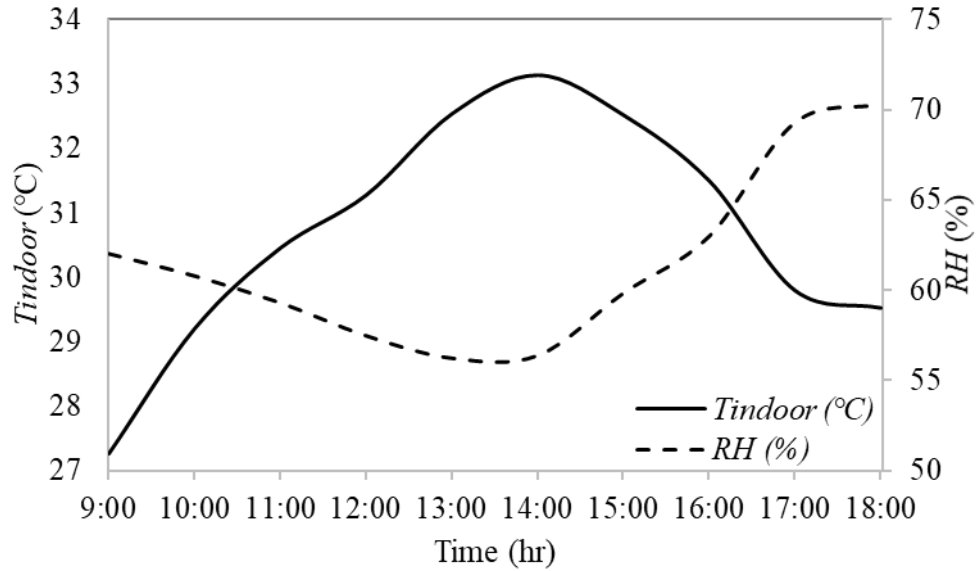


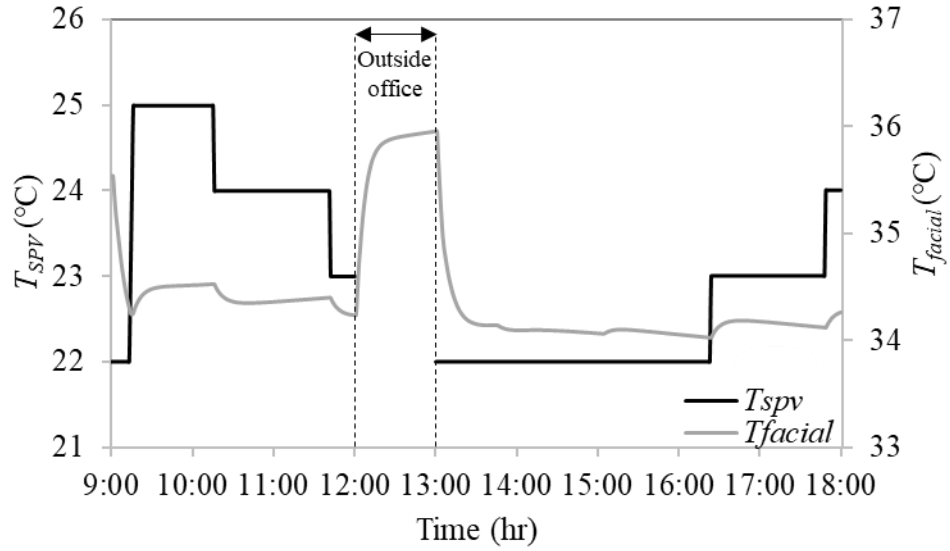
Fig. 16. Indoor conditions (T_{indoor} and RH) over the working hours for the month of August

In what follows, a discussion of the results for the considered case study is presented in detail. At 9:00 AM, the occupant enters the office space at a high metabolic rate of 2 met feeling slightly uncomfortable at a relatively low T_{indoor} of 27.28 °C with elevated T_{facial} of 35.54 °C, as shown in **Fig. 16** and **Fig. 17(a)**. The dynamic controller then automatically sets T_{SPV} to its minimum value of 22 °C causing a quick improvement in TC , as shown in **Fig. 17(b)**. Meanwhile, the occupant being seated, the metabolic rate starts decreasing to 1 met, and a drop in T_{facial} occurs to reach 34.30°C within 13 minutes. After that, the controller increases T_{SPV} with an increment of 1°C per minute to reach $T_{SPV.set}$ of 25°C causing a slight overshoot in TC . During the first few minutes, the controller

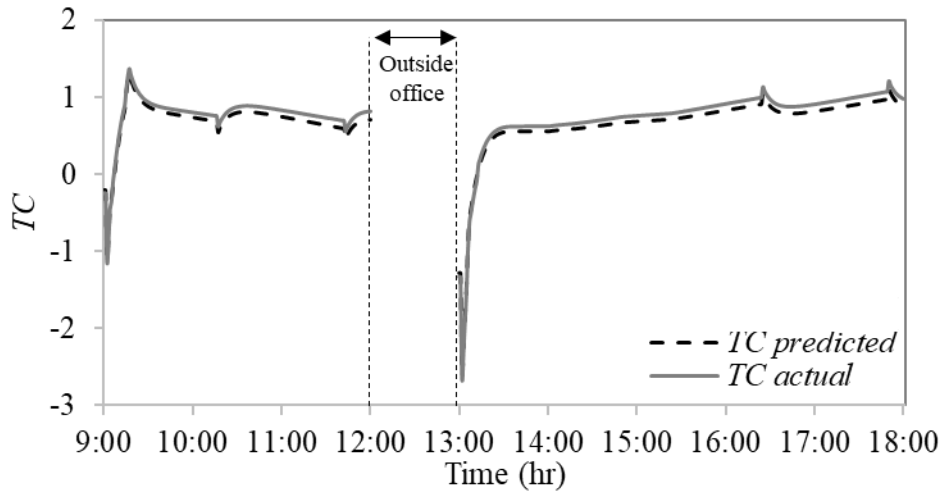
was allowed to overshoot to avoid unfeasible fluctuations in T_{SPV} , which explains why TC exceeded the limit of 1, as shown in **Fig. 17(b)**. The PV controller maintains a T_{SPV} of 25 °C for 1 hour causing an increase in T_{facial} to 34.53 °C, while maintaining TC around 0.7. Beyond 10:15 AM and with the increase in T_{indoor} , as shown in **Fig. 16**, T_{SPV} starts to decrease gradually reaching first 24°C then 23°C when T_{indoor} reaches 30.85 °C. At 12 PM, the occupant leaves the office (metabolic rate increases to 2 met) and comes back at 1 PM feeling very uncomfortable at T_{indoor} of 33.22 °C with an elevated T_{facial} of 35.95 °C. The PV automatically turns on at 22 °C, keeping it constant for the next 3 hours, improving TC to almost 0.91 and decreasing T_{facial} to 34.03 °C. To preserve TC between 0.5 and 1 for the remaining working hours with decreasing T_{indoor} , the PV controller gradually increases T_{SPV} to 23°C for the next 1 hour and to 24°C for the last 12 minutes maintaining TC and T_{facial} around 0.87 and 34.26°C, respectively, for T_{indoor} around 29.55°C.

Overall, the PV controller succeeded in attaining the target TC level between 0.5 and 1 at operation time for a typical hot and humid summer month. The predicted TC had similar values compared to the actual TC levels throughout the working period with a maximum deviation of 0.1, as shown in **Fig. 17(b)**. The recommended T_{SPV} was mainly affected by the transients of indoor conditions, transients in metabolic rate and by changes in T_{facial} . To this end, the designed controller responds properly under moderate hot and humid indoor conditions that are within the constraints and applicability of the developed TC correlation. The maximum TC level that the controller can attain under such conditions is 1, given that the range of T_{SPV} operation is between 22 and 26°C. The

occupant can always adjust the PV flow rate, if needed, to reach improved comfort states beyond 1.



(a)



(b)

Fig. 17. (a) The variation in T_{SPV} as well as T_{facial} and (b) the comparison between the predicted and the actual TC for a typical working day of August

CHAPTER VII

CONCLUSION

Real time access to an occupant's dynamic TC allows PV system controllers to continuously adjust their operational settings, while maintaining acceptable TC levels. Infrared thermography can be used to provide real time information about individuals' TC by constantly tracking T_{facial} and its rate of change, which proved to be strong indicators for TC . In this paper, an autonomously controlled PV unit is developed in a NV office space to ensure an acceptable TC between 0.5 and 1 with T_{indoor} that ranges between 25 and 33 °C, and RH between 60 and 80%. Regression equation that estimate TC was used. The dynamic NV-PV controller adjusts T_{SPV} based on predicted TC obtained from the adopted mathematical correlation. The developed controller is implemented in a case study scenario of an office space in Beirut's moderate hot and humid climate, and its performance is evaluated in attaining TC using direct simulations of the bioheat model. The developed controller is shown to achieve its goals in dynamically adjusting T_{SPV} and ensuring an acceptable TC of the occupant at all times of operation. The implementation of such autonomous PV units in office spaces is important for energy saving and ensuring TC for each occupant. The PV controller responds correctly only under a specific range of indoor temperatures and RH as well as metabolic rates. This means that at more elevated indoor conditions and metabolic rates, a new regression model should be established based on the new ranges. Future work may address the success of the system outside the considered range of this study along with experimental testing. Besides,

energy savings associated with the developed control over a full season of operation in comparison with conventional control methods of operation can be addressed.

BIBLIOGRAPHY

- [1] Ghahramani, Ali, Guillermo Castro, Simin Ahmadi Karvigh, and Burcin Becerik-Gerber. 2018. "Towards unsupervised learning of thermal comfort using infrared thermography." *Applied Energy* 211: 41-49.
- [2] Jazizadeh, Farrokh, and Wooyoung Jung. "Personalized thermal comfort inference using RGB video images for distributed HVAC control." *Applied Energy* 220 (2018): 829-841.
- [4] Cosma, Andrei Claudiu, and Rahul Simha. "Thermal comfort modeling in transient conditions using real-time local body temperature extraction with a thermographic camera." *Building and Environment* 143 (2018): 36-47.
- [6] Chen, Yixing, Chandra Sekhar, Kwok Wai Tham, and Benny Raphael. "Personalized Ventilation Control: Perception of Indoor Air Quality." In *10th REHVA World Congress*, vol. 9. 2010.
- [7] Melikov, Arsen Krikor. "Personalized ventilation." *Indoor air* 14 (2004): 157-167.
- [8] Melikov, Arsen K., Radim Cermak, and Milan Majer. "Personalized ventilation: evaluation of different air terminal devices." *Energy and buildings* 34, no. 8 (2002): 829-836.
- [9] Schiavon, Stefano, and Arsen K. Melikov. "Energy-saving strategies with personalized ventilation in cold climates." *Energy and Buildings* 41, no. 5 (2009): 543-550.

- [11] Nomura, Mika, and Kyosuke Hiyama. "A review: Natural ventilation performance of office buildings in Japan." *Renewable and Sustainable Energy Reviews* 74 (2017): 746-754.
- [12] Yang, T. O. N. G., and DEREK J. Clements-Croome. "Natural ventilation in built environment." *Sustainable Built Environments* 394425 (2013).
- [13] Khalil, Safaa, Kamel Ghali, Nesreen Ghaddar, and Mariam Itani. "Hybrid mixed ventilation system aided with personalised ventilation to attain comfort and save energy." *International Journal of Sustainable Energy* (2020): 1-18.
- [14] Taheri, Mahnameh, Matthias Schuss, Alfred Fail, and Ardeshir Mahdavi. "A performance assessment of an office space with displacement, personal, and natural ventilation systems." In *Building Simulation*, vol. 9, no. 1, pp. 89-100. Tsinghua University Press, 2016.
- [18] Hui, Z., 2003. Human thermal sensation and comfort in transient and non-uniform thermal environments. Unpublished doctoral dissertation, University of California, Berkeley.
- [19] Burzo, Mihai, Cakra Wicaksono, Mohamed Abouelenien, Veronica Perez-Rosas, Rada Mihalcea, and Yong Tao. "Multimodal sensing of thermal discomfort for adaptive energy saving in buildings." *iiSBE NET ZERO BUILT ENVIRONMENT* 344 (2014).
- [20] Ranjan, Juhi, and James Scott. 2016. "ThermalSense: determining dynamic thermal comfort preferences using thermographic imaging." In *Proceedings of the 2016 ACM International Joint Conference on Pervasive and Ubiquitous Computing* 1212-1222.

- [22] Keblawi, A., N. Ghaddar, and K. Ghali. 2011. "Model-based optimal supervisory control of chilled ceiling displacement ventilation system." *Energy and Buildings* 43 (6): 1359-1370.
- [25] Al Assaad, Douaa, Carine Habchi, Kamel Ghali, and Nesreen Ghaddar. "Simplified model for thermal comfort, IAQ and energy savings in rooms conditioned by displacement ventilation aided with transient personalized ventilation." *Energy Conversion and Management* 162 (2018): 203-217.
- [26] Itani, Mariam, Nesreen Ghaddar, Kamel Ghali, Djamel Ouahrani, and Beatrice Khater. "Significance of PCM arrangement in cooling vest for enhancing comfort at varied working periods and climates: Modeling and experimentation." *Applied Thermal Engineering* 145 (2018): 772-790.
- [27] Itani, Mariam, Rana Bachnak, Nesreen Ghaddar, and Kamel Ghali. "Evaluating performance of hybrid PCM-fan and hybrid PCM-desiccant vests in moderate and hot climates." *Journal of Building Engineering* 22 (2019): 383-396.
- [28] Metzmacher, Henning, Daniel Wölki, Carolin Schmidt, Jérôme Frisch, and Christoph van Treeck. "Real-time human skin temperature analysis using thermal image recognition for thermal comfort assessment." *Energy and Buildings* 158 (2018): 1063-1078.
- [33] Melikov, Arsen Krikor, M. A. Skwarczynski, J. Kaczmarczyk, and J. Zabecky. "Use of personalized ventilation for improving health, comfort, and performance at high room temperature and humidity." *Indoor Air* 23, no. 3 (2013): 250-263.

- [34] Veselý, Michal, and Wim Zeiler. "Personalized conditioning and its impact on thermal comfort and energy performance—A review." *Renewable and Sustainable Energy Reviews* 34 (2014): 401-408.
- [36] Al Assaad, Douaa, Kamel Ghali, and Nesreen Ghaddar. "Effectiveness of intermittent personalized ventilation assisting a chilled ceiling for enhanced thermal comfort and acceptable indoor air quality." *Building and Environment* 144 (2018): 9-22.
- [39] Al-Othmani, M., N. Ghaddar, and K. Ghali. "A multi-segmented human bioheat model for transient and asymmetric radiative environments." *International Journal of Heat and Mass Transfer* 51, no. 23-24 (2008): 5522-5533.
- [40] De Dear, Richard J., Edward Arens, Zhang Hui, and Masayuki Oguro. "Convective and radiative heat transfer coefficients for individual human body segments." *International Journal of Biometeorology* 40, no. 3 (1997): 141-156.
- [41] Solutions, I. E. "Introducing IESVE Software." Online at <http://www.iesve.com/software> (2020).
- [43] Al Assaad, Douaa, Kamel Ghali, and Nesreen Ghaddar. "Effect of flow disturbance induced by walking on the performance of personalized ventilation coupled with mixing ventilation." *Building and Environment* 160 (2019): 106217.
- [44] Karaki, Wafaa, Nesreen Ghaddar, Kamel Ghali, Kalev Kuklane, Ingvar Holmér, and Leif Vanggaard. "Human thermal response with improved AVA modeling of the digits." *International journal of thermal sciences* 67 (2013): 41-52.
- [51] Zhu, Shengwei, Shinsuke Kato, Doosam Song, Shuzo Murakami, and Mine Sudo. "Study on the personal air-conditioning system considering human thermal

- adaptation." In Proceedings of 4th International Symposium on HVAC, Beijing, China, October, pp. 9-11. 2003.
- [52] Boerstra, A. C., M. G. L. C. Loomans, and J. L. M. Hensen. "Personal control over indoor climate and productivity." In 13th International Conference on Indoor Air Quality and Climate (Indoor Air 2014), June 7-12, 2014, Hong Kong, pp. 1-8. ISIAQ, 2014.
- [53] Hoyt, T., S. Schiavon, A. Piccioli, T. Cheung, D. Moon, and K. Steinfeld. "CBE thermal comfort tool center for the built environment." University of California Berkeley. Available online: <http://comfort.cbe.berkeley.edu> (accessed on 14 July 2020) (2013).
- [55] Annan, Ghina, Nesreen Ghaddar, and Kamel Ghali. "Natural ventilation in Beirut residential buildings for extended comfort hours." *International Journal of Sustainable Energy* 35, no. 10 (2016): 996-1013.
- [57] Aryal, Ashrant, and Burcin Becerik-Gerber. "A comparative study of predicting individual thermal sensation and satisfaction using wrist-worn temperature sensor, thermal camera and ambient temperature sensor." *Building and Environment* 160 (2019): 106223.
- [59] Wasserman, Larry. *All of statistics: a concise course in statistical inference*. Springer Science & Business Media, 2013.
- [60] Massimiliano, Bonamente. "Statistics and Analysis of Scientific Data." (2013). Birmingham, AL: Springer.

- [61] Gardezi, Syed Shujaa Safdar, Nasir Shafiq, Noor Amila Wan Abdullah Zawawi, Muhd Faris Khamidi, and Syed Ahmad Farhan. "A multivariable regression tool for embodied carbon footprint prediction in housing habitat." *Habitat International* 53 (2016): 292-300.
- [62] Qiang, Guo, Tian Zhe, Ding Yan, and Zhu Neng. "An improved office building cooling load prediction model based on multivariable linear regression." *Energy and Buildings* 107 (2015): 445-455.
- [65] Alsaad, Hayder, and Conrad Voelker. "Performance assessment of a ductless personalized ventilation system using a validated CFD model." *Journal of Building Performance Simulation* 11, no. 6 (2018): 689-704.
- [66] van Treeck, Christoph, Jérôme Frisch, Michael Pfaffinger, Ernst Rank, Stefan Paulke, Iris Schweinfurth, Rudolf Schwab, Runa Hellwig, and Andreas Holm. "Integrated thermal comfort analysis using a parametric manikin model for interactive real-time simulation." *Journal of Building Performance Simulation* 2, no. 4 (2009): 233-250.
- [67] Cropper, Paul C., Tong Yang, Malcolm Cook, Dusan Fiala, and Rehan Yousaf. "Coupling a model of human thermoregulation with computational fluid dynamics for predicting human–environment interaction." *Journal of Building Performance Simulation* 3, no. 3 (2010): 233-243.
- [68] Barstow, Thomas J., and Paul A. Molé. "Linear and nonlinear characteristics of oxygen uptake kinetics during heavy exercise." *Journal of Applied Physiology* 71, no. 6 (1991): 2099-2106.

- [69] Zhang, Jianxin, et al. "Design of PID Temperature Control System Based on STM32." *IOP Conference Series. Materials Science and Engineering*, vol. 322, 2018, pp. 72020.
- [70] C. Huizenga, S. Abbaszadeh, L. Zagreus, E.A. Arens, Air quality and thermal comfort in office buildings: results of a large indoor environmental quality survey, *Proceedings of Healthy Buildings III (2006)* 393–397.
- [71] Shan, Chengcheng, et al. "Towards Non-Intrusive and High Accuracy Prediction of Personal Thermal Comfort using a Few Sensitive Physiological Parameters." *Energy & Buildings*, vol. 207, 2020, pp. 109594.
- [72] D. Daum, F. Haldi, N. Morel, A personalized measure of thermal comfort for building controls, *Build. Environ.* 46 (1) (2011) 3–11.
- [73] M.A. Humphreys, J.F. Nicol, The validity of ISO-PMV for predicting comfort votes in every-day thermal environments, *Energy Build.* 34 (6) (2002) 667–684.
- [74] J. Gonzalez-Alonso, Human thermoregulation and the cardiovascular system, *Exp. Physiol.* 97 (3) (2012) 340–346.
- [75] B. Pavlin, G. Pernigotto, F. Cappelletti, P. Bison, R. Vidoni, A. Gasparella, Real-time monitoring of occupants' thermal comfort through infrared imaging: a preliminary study, *Buildings* 7 (1) (2017), <http://dx.doi.org/10.3390/buildings7010010> <http://www.mdpi.com/2075-5309/7/1/10>.

- [79] Song, Jia-liang, et al. "Study on PID Temperature Control Performance of a Novel PTC Material with Room Temperature Curie Point." *International Journal of Heat and Mass Transfer*, vol. 95, 2016, pp. 1038-1046.
- [82] Yao, Y., Huang, M., & Chen, J. (2013). State-space model for dynamic behavior of vapor compression liquid chiller. *International journal of refrigeration*, 36(8), 2128-2147.
- [83] Shi-Ming, D., & Missenden, J. F. (1999). Applying classical control theory for validating and simplifying a dynamic mathematical model of an air-conditioning plant. *ASHRAE Transactions*, 105, 140.
- [84] Salloum, M., Ghaddar, N. and Ghali, K., 2007. A new transient bioheat model of the human body and its integration to clothing models. *International journal of thermal sciences*, 46(4), pp.371-384.
- [85] Doctor-Pingel, M., Vardhan, V., Manu, S., Brager, G. and Rawal, R., 2019. A study of indoor thermal parameters for naturally ventilated occupied buildings in the warm-humid climate of southern India. *Building and Environment*, 151, pp.1-14.
- [86] Jin, Q., Duanmu, L., Zhang, H., Li, X. and Xu, H., 2011. Thermal sensations of the whole body and head under local cooling and heating conditions during step-changes between workstation and ambient environment. *Building and environment*, 46(11), pp.2342-2350.

APPENDIX A

Testing of the NV-PV controller with the adopted T_{SPV} rate of change

The adopted rate of T_{SPV} change of 1 °C for every 0.3 °C difference in facial temperature was tested using two extreme cases of T_{indoor} . The results should imply that the NV-PV controller can change T_{SPV} to maintain TC in the acceptable range of 0.5 and 1 in both cases. The cases consider a person with a metabolic rate of 2 met in indoor conditions of $T_{indoor} = 33$ °C for case 1 ($T_{indoor} = 25$ °C for case 2) and $RH = 70$ %. The resultant TC status is not comfortable. Then, the person enters a space at the same indoor conditions but gets seated with a metabolic rate of 1 met for one hour. In order to attain TC , the NV-PV controller should change T_{SPV} according to the TC status, starting from an initial value of 22°C for a one-hour period.

Fig. 18 shows the transient T_{SPV} and TC results of testing the rate of T_{SPV} change at T_{indoor} of (a) 33 °C and (b) 25 °C. The difference in the response of the controller between the two extreme cases can be clearly seen. For case 1 with $T_{indoor} = 33$ °C, **Fig. 18 (a)**, the controller did not vary T_{SPV} for the whole hour and kept it at its minimum of 22 °C. This is in accordance with the corresponding TC level that started with a value of -4, which is a very uncomfortable state, and then increased due to PV operation. The TC improved as desired and reached a value of 0.53, which is close to the lower acceptable TC limit of 0.5. On the other hand, for case 2 with $T_{indoor} = 25$ °C, **Fig. 18 (b)**, the controller kept T_{SPV} at 22 °C for the first 6 minutes, due to the uncomfortable state with $TC = -0.9$. Accordingly, TC improved to 0.59, after which the controller increased T_{SPV} to 23 °C and then to 24 °C in the next 2 minutes. This happened since the metabolic rate is dropping

from 2 to 1 met, while T_{indoor} of 25 °C is relatively acceptable at typical office conditions. After 19 minutes, TC was about 0.6 and the controller increased T_{SPV} to 25 °C for the remaining time, where TC stabilized at 0.57. Both cases showed how the NV-PV controller was able to react with the adopted rate of T_{SPV} change to quickly attain TC , and change T_{SPV} to maintain TC in the acceptable range.

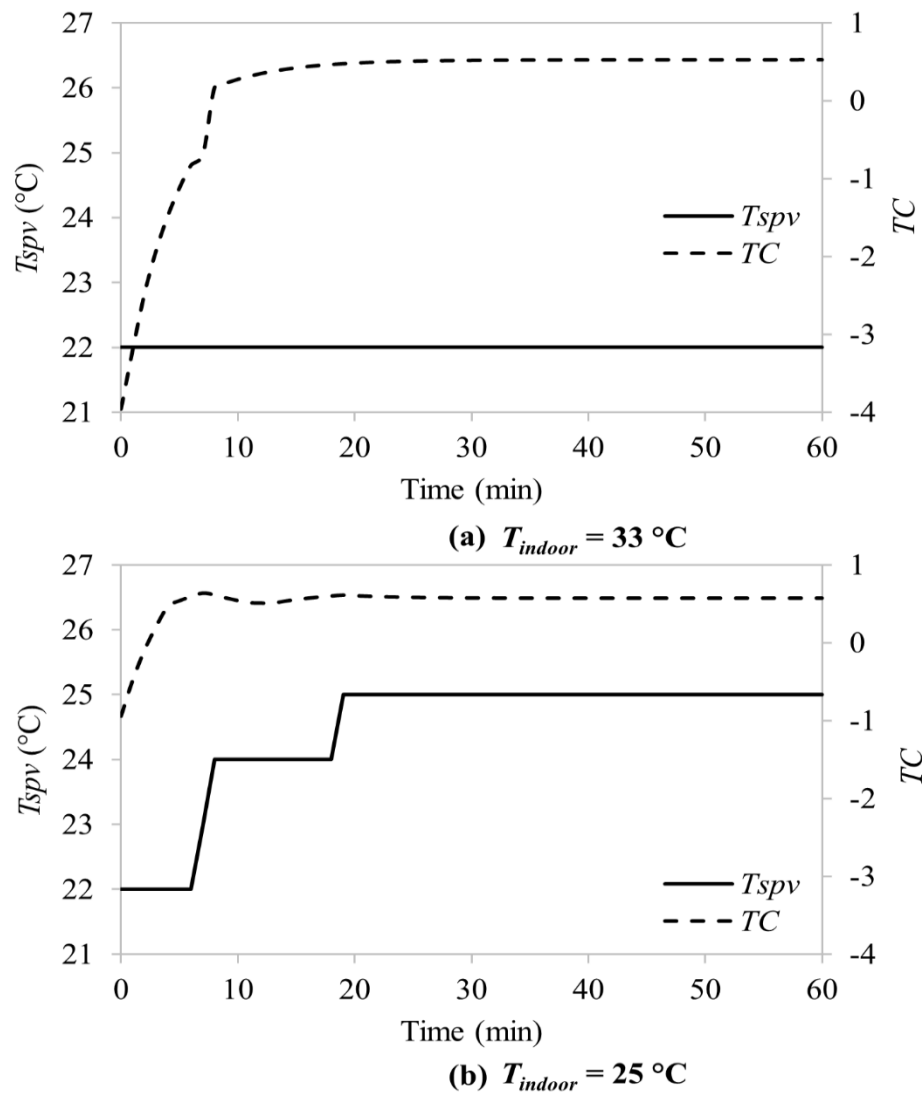


Fig. 18. Transient T_{SPV} and TC results of testing the rate of T_{SPV} change at T_{indoor} of (a) 33 °C and (b) 25 °C